Kent Academic Repository

Clark, Ewan R. and Borys, Andryj M (2017) *Adducts of Donor—Functionalized Ar3P with the Soft Lewis—Acid I2: Probing Simultaneous Lewis Acidity and Basicity at Internally Solvated P(III) Centers.* Inorganic Chemistry, 56 (8). pp. 4622-4634. ISSN 0020-1669.

Adducts of donor-functionalised Ar$_3$P with the soft Lewis acid I$_2$ – Probing simultaneous Lewis acidity and basicity at internally solvated P(III) centres

Andryj M. Borys, Ewan R. Clark[*]

School of Physical Sciences, Ingram Building, University of Kent, Canterbury, CT2 7NH.

Abstract

The enhancement of donor strength of *ortho*-functionalised triarylphosphanes is shown to occur *via* different mechanisms for O- and N- donor substituents, with internal solvation of the phosphorus centre observed for N-donors. Nevertheless, the steric congestion about the P-centre is shown to significantly oppose the increase in donor ability, leading to weaker donation than expected. A series of *mono-* and *bis*-aryl substituted Ar$_3$PI$_2$ adducts [Ph$_{3-n}$(*o*-OMe-C$_6$H$_4$)$_n$PI$_2$, Ph$_{3-n}$(*o*-NMe$_2$-C$_6$H$_4$)$_n$PI$_2$, Ph$_{3-n}$(*o*-CH$_2$NMe$_2$-C$_6$H$_4$)$_n$PI$_2$ (*n* = 1,2)] have been synthesized *via* the 1:1 reaction of donor-functionalized phosphanes with diiodine. These soft Lewis acid/base adducts exhibit apparent internal solvation of the donor phosphorus by the pendant donor moieties giving rise to five- or six-coordinate phosphorus atoms acting as both Lewis base and Lewis acid; the first neutral six-coordinate simultaneous P(III) Lewis acid and Lewis base adduct is reported. Single crystal X-ray diffraction studies reveal unexpectedly weak donor strength for one of the phosphanes, indicating significant steric hindrance as a

consequence of internal solvation. Crystallographic interrogation of the corresponding iodophosphonium salts [Ar$_3$PI]X (X = I$_3$, BAr^F) shows that the cationic complexes experience a still greater influence of the steric bulk of the donor moieties than their neutral precursors. The steric and electronic contributions to bonding have been analysed through computational studies, determining the factors governing the basicity of these donor-functionalised phosphanes, and show that enhancement of P-centred donor strength occurs by conjugation of lone pairs through the arene rings for oxygen substituents, and *via* internal solvation for the nitrogen donors.

Introduction

The Lewis acidity of main group species may be modulated by choice of substituents and overall charge, leading to exploitable reactivities. Work by Stephan,[1] Ingleson,[2] and Crudden[3] has shown that appropriately substituted and stabilised borenium cations are able to activate dihydrogen, in some cases catalytically, and Stephan has successfully extended this to catalysis by phosphonium cations.[4] Hudnall[5] and Gabbaï[6] have exploited stibonium cations as Lewis acids to activate aldehydes, and Alcarazo has used carbene stabilised sulfenyl cations to mimic the reactivity of λ-3 iodanes, leading to new C-C bond forming reactions.[7] In all cases, careful choice of substituents was key to controlling reactivity, and the nature of the interaction of main group Lewis acids with donor species is therefore of fundamental importance. We recently reported that, counter to expectations, the phosphanes **1a-1c** bearing *ortho*-donor functionality to permit chelation, form less stable phosphane-phosphenium adducts with the diphenylphosphenium cation than the unsubstituted base triphenylphosphane.[8] Computational studies, coupled with the crystallographic characterisation of [**1c**.PPh$_2$]BAr^F, showed that the donor phosphanes adopted an internally coordinated configuration, raising the energy of the phosphorus lone pairs, but nevertheless produced less stable adducts, implying significant steric influence on complex

stability. This is in marked contrast with the behaviour of these phosphanes in transition metal complexes, wherein they behave as chelate ligands,[9] or with hard main group Lewis acids, where competitive binding with the donor functionality is observed.[10] Diiodophosphoranes, which may be regarded as phosphane-diiodine Lewis adducts, are highly crystalline species and so were selected as suitable targets to provide structural information on the behaviour of these phosphanes with soft, low steric demand Lewis acids.
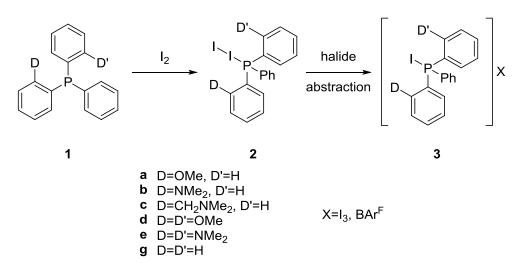
The solid-state structures of dihalophosphoranes of the formula R_3PX_2 (X = F, Cl, Br, I) have been established for many years and whilst five-coordinate molecular trigonal bypyramidal species, R_3PX_2, and ionic halo-phosphonium salts, $[R_3PX]X$, are most common for the more electronegative elements X = F,[11] Cl[12-15] and Br[16-18], charge-transfer (CT) compounds with a molecular "spoke" structure, R₃P-X-X, dominate for diiodine[19-22] adducts (this structure has also been observed for X = Br[16,21]). Intermediate forms in which concatenation leads to [Ar₃P-XXX-PAr₃]X are known for X = Cl and Br, highlighting the covalent nature of bonding in these systems.[23,24]

The CT "spoke" structure may be understood as P(III) Lewis acid/base adducts of the very soft, linear Lewis acid diiodine, with the limiting structure of iodophosphonium iodides with strong cation-anion interactions between the phosphorus-bound iodine centre and the iodide anion. Regardless of the interpretation, it has been established that the P-I and I-I bond lengths of the spoke structure are highly sensitive to both the steric demand about the phosphorus centre and its electron donating capacity.[21,25] The length of the I-I interaction varies considerably and almost continuously between 3.021(1) Å[26] for $(\text{Mecarb})^i\text{Pr}_2\text{PI}_2$ [Me-carb = 1-(2-Me-1,2-C₂B₁₀H₁₀)] and 3.6389(14) Å[27] for $[(^n\text{Pr}_2\text{N})_3\text{PI}]\text{I}$, significantly longer than the I-I bond lengths observed in Ph_3AsI_2 (3.005(1) Å)[28] and I_2 (2.660 Å)[29], but still within the sum of the Van der Waals radii

(3.96 Å).[30] This lengthening of the I-I bond occurs as electron density is transferred into the σ* orbital of diiodine by the electron donor, R_3P. Consequently, the I-I distances can be regarded as highly indicative of the degree of charge transfer and thus donor strength.

Steric effects also play a significant role in influencing the magnitude of the P-I and I-I bond lengths. In particular, the P-I distances show greater susceptibility to steric influence than the I-I contacts. This phenomenon becomes readily apparent when regarding the aryl groups in Ar_3PI_2 adducts, since the conformation adopted by aryl groups and orientation of any substituents has a major impact on the steric properties. For instance, the P-I and I-I bond metrics for *tris*-(*m*-tolyl)- and *tris*-(*p*-tolyl)-diiodophosphorane [2.479(3)-2.472(5) Å /3.1809(17)-3.1815(15) Å][31] are essentially identical, with the P-I contact equivalent within errors to Ph_3PI_2[32] [2.4690(8) Å], but with a significant increase in I-I separation [*cf.* 3.161(2) Å] due to the greater electron donating capacity of the tolyl-groups. In contrast, the *tris*-(*o*-tolyl)-diiodophosphorane[33] shows a dramatically longer P-I contact [2.5523(12) Å] and a concomitant decrease in the I-I separation [3.0727(4) Å]. Further studies into *tris*-aryl substituted Ar_3PI_2 adducts by Barnes[25] show that electronic effects are primarily responsible for differences in the bond lengths in *m*- and *p*-substituted Ar_3PI_2 adducts, whilst steric effects become of significant importance for *o*-substituted adducts. Donor *ortho*-substituents have been shown to have a significant impact on the reaction kinetics of both phosphane alkylation and the alkaline decomposition of the subsequent phosphonium salts.[34,35] Both *ortho*-OMe and *ortho*-NMe_2 functionality leading to increase in rate of alkylation, attributed to internal coordination of the donor to phosphorus, but nevertheless show starkly different decomposition behaviour, with the O-donor species undergoing slower P-C bond cleavage than PPh_3 derivatives,[36] whilst the N-donor species is decomposed at an enhanced rate.[35]

In this report, we describe the synthesis of a family (Scheme 1) of simple donor-functionalized diiodophosphoranes and their iodophosphonium salts from ubiquitous triarylphosphane ligands. The result of *ortho*-donor substitution on their Lewis basicity is discussed in terms of steric and electronic effects with the aid of computational studies, and it is shown that *ortho*-nitrogen and oxygen donors contribute to the donor strength of the phosphane by different mechanisms.

a D=OMe, D'=H
b D=NMe$_2$, D'=H
c D=CH$_2$NMe$_2$, D'=H
d D=D'=OMe
e D=D'=NMe$_2$
g D=D'=H

X=I$_3$, BAr^F

Scheme 1: Donor-functionalised diiodophosphoranes and iodophosphonium salts prepared in this report.

Experimental

General Experimental

The syntheses of diiodophosphoranes and iodophosphonium salts described herein were undertaken using standard Schlenk techniques under anhydrous and anaerobic conditions. All solvents were purchased from Fisher Scientific and dried before use using the methods specified. DCM was dried using an Innovation Technologies Benchtop Solvent Purification System and stored over activated molecular sieves. THF was dried by reflux over potassium and stored over activated molecular sieves. ^{n}Hexane and diethyl ether were dried by reflux over sodium/benzophenone and stored over potassium mirrors. ^{n}Butyl-lithium was purchased from

Acros as a 2.5M solution in hexanes. Sodium tetrakis(3,5-trifluoromethylphenyl)borate (NaBAr^F) was sourced from Matrix Scientific and washed with DCM prior to use. Ph$_2$PCl and PhPCl$_2$ were distilled prior to use and stored in flame-dried ampoules under argon. All other compounds were used as supplied by the manufacturer. The donor phosphanes were synthesised using the method previously reported.[8] NMR spectra were recorded on a JEOL 400 MHz NMR Spectrometer and spectra referenced to the appropriate residual solvent peaks.

Crystallography

Diffraction data were recorded on Agilent Super Nova Dual Diffractometers with Mo-Kα radiation (λ = 0.71073 Å) or Cu-Kα (λ = 1.54184 Å) at 100 K. Single crystals were mounted on nylon cryoloops or MiTeGen microloops. Unit cell determination, data reduction and absorption corrections were carried out using CrysAlisPro 38.41. Using the Olex2 GUI[37], the structure was solved with the ShelXT[38] structure solution program via Direct Methods and refined with the ShelXL[39] refinement package using Least Squares minimization. Non-hydrogen atoms were refined anisotropically and hydrogen atoms were included using a riding model. All thermal ellipsoid plots were generated using ORTEP-3 for Windows.[40] Details of the crystal habits and data collection may be found in the SI.

Computational Work

Calculations were performed using the Gaussian09[41] suite of programs. Structures were optimised from single crystal X-ray diffraction data using the M06-2X hybrid functional[42] using the def2TZVP[43] split valence, triple zeta basis set to describe the iodine atoms and 6-311g(d,p)[44] for all other atoms; PCM (Dichloromethane) solvation was used in all cases,[45] and all structures were confirmed as minima by frequency analysis and the absence of imaginary frequencies. NBO calculations and NBO Wiberg Bond Index determinations were performed using NBO

3.1.;[46] Mayer Bond Indices[47,48] were calculated using Multiwfn 3.3.9.[49] The Mayer bond indices were found to show stronger correlation between changes in bond index and bond length than the NAO-adjusted Wiberg Bond Indices and so were used in subsequent analysis. Full Cartesian coordinates for the optimised geometries are provided in the supporting information.

Syntheses

Synthesis of Diiodophosphoranes

The Ar_3PI_2 adducts **2a-2e** and **2g** were all prepared by the reaction of donor-functionalized phosphane with one equivalent of diiodine in anhydrous diethyl ether. The synthesis of **2a** is given as exemplar. All products were isolated as free flowing yellow powders. Crystals suitable for single crystal X-ray diffraction were grown by slow diffusion of Et_2O into a concentrated solution of the product in DCM. Where necessary, products were purified by recrystallization from DCM and Et_2O. In the case of **2c**, we were unable to isolate the compound free of *c.a.* 25% phosphine oxide impurity identified by NMR despite repeated recrystallisation, suggesting extreme moisture sensitivity and concomitant crystallisation. A sample of **2g** was synthesised for crystallographic comparison and the NMR spectra were found to match literature values.[20]

Synthesis of [Ph₂P(*o*-OMe-C₆H₄)]I₂ [2a] : To a stirred solution of **1a** (200 mg, 0.684 mmol) in Et_2O (10 cm³) was added dropwise a solution of I_2 (165 mg, 0.650 mmol) in Et_2O (10 cm³), generating an immediate yellow precipitate. The reaction mixture was stirred overnight, the pale yellow supernatant removed by filtration and the solid product washed with Et_2O (10 cm³) before being dried *in vacuo* to give the product as a bright yellow powder (247 mg, 0.453 mmol, 70% yield). Crystals suitable for single crystal diffraction were grown by slow diffusion of Et_2O into a

concentrated solution of product in DCM. *Anal.* Calc. for $C_{19}H_{17}I_2OP$: C, 41.79; H, 3.14. Found: C, 41.89; H, 3.17. **^{1}H NMR** (400 MHz, DCM, 20.9 °C): δ = 7.76-7.67 (bm, 3H, *Ph*), 7.59-7.55 (m, 8H, *Ph*), 7.14-7.06 (m, 2H, *Ph*), 6.98 (dd, *J* = 14.7, 7.8 Hz, 1H, *Ph*), 3.76 (s, 3H, O*Me*). **^{31}P NMR** (161.8 MHz, DCM, 20.9 °C): δ = -24.4 (s). **^{13}C{^{1}H} NMR** (100.5 MHz, DCM, 19.3 °C): δ = 161.7 (d, J_{C-P} = 1.9 Hz, *Ph*), 137.2 (d, J_{C-P} = 1.9 Hz, *Ph*), 135.0 (d, J_{C-P} = 5.8 Hz, *Ph*), 133.9 (d, J_{C-P} = 2.9 Hz, *Ph*), 133.4 (d, J_{C-P} = 10.5 Hz, *Ph*), 127.9 (d, J_{C-P} = 10.5 Hz, *Ph*), 122.6 (d, J_{C-P} = 65.2 Hz, *Ar*-P), 121.8 (d, J_{C-P} = 12.5 Hz, *Ph*), 112.7 (d, J_{C-P} = 6.7 Hz, *Ph*), 109.3 (d, J_{C-P} = 64.0 Hz, *Ar*-P), 65.1 (s, O*Me*). **SCXRD** P-1, a 8.7185(3) Å, b 9.8085(3) Å, c 11.5663(3) Å, α 94.431(2) °, β 95.603(2) °, γ 104.837(2) °, R_1/wR_2 0.0210/0.0407.

Synthesis of [Ph$_2$P(*o*-NMe$_2$-C$_6$H$_4$)]I$_2$ [2b]: (yellow solid, 85% yield). *Anal.* Calc. for $C_{20}H_{20}I_2NP$: C, 42.96; H, 3.61; N, 2.50. Found: C, 42.92; H, 3.73; N, 2.65. **^{1}H NMR** (400 MHz, DCM, 20.5 °C): δ = 7.76 (t, *J* = 7.3 Hz, 1H, *Ph*), 7.65-7.50 (m, 11H, *Ph*), 7.35 (dt, *J* = 2.7, 7.8 Hz, 1H, *Ph*), 7.18 (dd, *J* = 7.8, 13.3 Hz, 1H, *Ph*), 2.24 (s, 6H, N*Me$_2$*). **^{31}P NMR** (161.8 MHz, DCM, 20.5 °C): δ = -25.8 (s). **^{13}C{^{1}H} NMR** (100.5 MHz, DCM, 20.5 °C): δ = 159.2 (d, J_{C-P} = 6.7 Hz, *Ph*), 136.3 (d, J_{C-P} = 2.9 Hz, *Ph*), 134.6 (d, J_{C-P} = 7.7 Hz, *Ph*), 133.6 (s, *Ph*), 133.5 (s, *Ph*), 133.4 (s, *Ph*), 129.6 (d, J_{C-P} = 11.5 Hz, *Ph*), 127.4 (d, J_{C-P} = 11.5 Hz, *Ph*), 126.5 (d, J_{C-P} = 7.7 Hz, *Ph*), 124.4 (d, J_{C-P} = 63.3 Hz, *Ar*-P), 122.7 (d, J_{C-P} = 67.0 Hz, *Ar*-P), 45.6 (s, N*Me$_2$*). **SCXRD** P-1, a 9.2731(3) Å, b 10.0341(3) Å, c 11.6573(3) Å, α 67.852(3) °, β 88.456(2) °, γ 84.209(2) °, R_1/wR_2 0.0153/0.0336.

Synthesis of [Ph$_2$P(*o*-CH$_2$NMe$_2$-C$_6$H$_4$)]I$_2$ [2c]: (yellow solid, converstion is quantitative by in situ NMR, but isolated samples were contaminated by phosphine oxide which could not be removed by recrystalisation). *Anal.* Calc. for $C_{21}H_{22}I_2NP$: C, 44.00; H, 3.87; N, 2.44. Found: C, 43.89; H, 3.95; N, 2.56. **^{1}H NMR** (400 MHz, DCM, 20.9 °C): δ = 7.75-7.34 (bm, 13H, *Ph*), 7.15

(dd, J = 7.3, 14.2 Hz, 1H, *Ph*), 3.57 (bs, 2H, CH_2NMe$_2$), 1.65 (bs, 6H. N*Me$_2$*). **^{31}P NMR** (161.8

MHz, DCM, 20.9 °C): δ = -23.1 (s). **^{13}C{^{1}H} NMR** (100.5 MHz, DCM, 18.1°C): δ = 145.8 (d,

J_{C-P} = 9.6 Hz, *Ph*), 135.4 (d, J_{C-P} = 4.8 Hz, *Ph*), 134.6 (d, J_{C-P} = 12.0 Hz, *Ph*), 134.0 (d, J_{C-P} = 7.2

Hz, *Ph*), 132.9 (d, J_{C-P} = 8.6 Hz, *Ph*),131.8 (d, J_{C-P} = 11.5 Hz, *Ph*), 129.5 (d, J_{C-P} = 11.5 Hz, *Ph*),

128.0 (d, J_{C-P} = 12.0 Hz, *Ph*), 125.8 (d, J_{C-P} = 62.8 Hz, *Ar*-P), 120.6 (d, J_{C-P} = 57.0 Hz, *Ar*-P),

59.4 (s, CH_2NMe$_2$), 43.8 (s, N*Me$_2$*). **SCXRD** P2$_1$/c, a 9.0359(3) Å, b 25.5171(7) Å, c 9.4963(3)

Å, α 90°, β 106.832(3) °, γ 90°, R$_1$/wR$_2$ 0.0233/ 0.0414.

Synthesis of [PhP(*o*-OMe-C$_6$H$_4$)$_2$]I$_2$ [2d]: (yellow solid, 85% yield). *Anal.* Calc. for

C$_{20}$H$_{19}$I$_2$O$_2$P: C, 41.69; H, 3.32. Found: C, 41.51; H, 3.36. **^{1}H NMR** (400 MHz, DCM, 19.7 °C):

δ = 7.73-7.50 (m, 7H, *Ph*), 7.12-7.04 (m, 6H, *Ph*), 3.77 (s, 6H, O*Me*). **^{31}P NMR** (161.8 MHz,

DCM, 20.0 °C): δ = -32.1 (s). **^{13}C{^{1}H} NMR** (100.5 MHz, DCM, 18.7 °C): δ = 161.6 (d, J_{C-P} =

2.9 Hz, *Ph*), 136.7 (d, J_{C-P} = 2.9 Hz, *Ph*), 134.8 (d, J_{C-P} = 6.7 Hz, *Ph*), 133.5 (d, J_{C-P} = 2.9 Hz,

Ph), 133.3 (d, J_{C-P} = 9.6 Hz, *Ph*), 129.4 (d, J_{C-P} = 13.4 Hz, *Ph*), 122.7 (d, J_{C-P} = 69.0 Hz, *Ar*-P),

121.6 (d, J_{C-P} = 12.5 Hz, *Ph*), 112.7 (d, J_{C-P} = 6.7 Hz, *Ph*), 109.2 (d, J_{C-P} = 67.1 Hz, *Ar*-P), 56.0

(s, O*Me*). **SCXRD** P-1, a 8.76192(19) Å, b 10.48116(19) Å, c 11.4220(3) Å, α 90.3592(17) °, β

94.2694(18) °, γ 95.4542(16) °, R$_1$/wR$_2$ 0.0172/ 0.0397.

Synthesis of [PhP(*o*-NMe$_2$-C$_6$H$_4$)$_2$]I$_2$ [2e]: (yellow solid, 81% yield). *Anal.* Calc. for C$_{22}$H$_{25}$I$_2$N$_2$P:

C, 43.88; H, 4.18; N, 4.65. Found: C, 43.77; H, 4.06; N, 4.62. **^{1}H NMR** (400 MHz, DCM, 18.7 °C): δ

= 7.83 (dd, J = 8.0, 15.3 Hz, 2H, *Ph*), 7.76 (t, J = 7.1, 7.3 Hz, 2H, *Ph*), 7.62-7.44 (m, 9H, *Ph*),

2.14 (s, 12H, N*Me$_2$*). **^{31}P NMR** (161.8 MHz, DCM, 19.2 °C): δ = -22.1 (s). **^{13}C{^{1}H} NMR** (100.5

MHz, DCM, 19.3 °C): δ = 158.7 (d, J_{C-P} = 3.8 Hz, *Ph*), 135.9 (d, J_{C-P} = 2.9 Hz, *Ph*), 135.5 (d, J_{C-P} = 9.6 Hz, *Ph*), 133.0 (d, J_{C-P} = 3.8 Hz, *Ph*), 132.3 (d, J_{C-P} = 9.6 Hz, *Ph*), 129.2 (d, J_{C-P} = 13.4

Hz, *Ph*), 127.4 (d, J_{C-P} = 13.4 Hz, *Ph*), 127.3 (d, J_{C-P} = 61.4 Hz, *Ar*-P), 125.9 (d, J_{C-P} = 7.7 Hz,

Ph), 121.9 (d, J_{C-P} = 72.9 Hz, *Ar*-P), 45.8 (s, N*Me₂*). **SCXRD** P2₁/c, a 8.94007(14) Å, b 42.9758(6) Å, c 12.85504(19) Å, α 90°, β 108.5752(17) °, γ 90 °, R₁/wR₂ 0.0246/ 0.0495.

Synthesis of 2g:[20,32] **SCXRD** P2₁2₁2₁, a 10.33101(9) Å, b 12.83882(12) Å, c 13.61886(13) Å, α 90°, β 90 °, γ 90 °, R₁/wR₂ 0.0162/ 0.0368.

Synthesis of Iodophosphonium Salts

NMR scale samples of the iodophosphonium BAr^F salts were prepared by the following general method unless otherwise stated: To a J. Young's NMR tube fitted with a d₆-DMSO capillary was added diiodophosphorane **2** (0.04 mmol) and DCM (0.7 cm³). NaBAr^F (0.04 mmol) was added and the reaction mixture was heated to reflux for 1 hour. The supernatant was decanted into a Schlenk flask equipped with a stir bar, and hexane (10 cm³) was added with stirring forming a precipitate that was subsequently filtered, washed with hexane (5 cm³) and dried *in vacuo*. Slow diffusion of hexane into a saturated solution of the product in DCM afforded single crystals suitable for X-ray diffraction. The same method was applied for the triiodide salts using diiodine, with diethyl ether as the anti-solvent. All reactions were monitored *via* NMR at each stage. See supporting information for further details.

Synthesis of [Ph₂P(*o*-OMe-C₆H₄)I][BAr^F] [3a]BAr^F: (off-white solid, 58% yield). *Anal.* Calc. for C₅₁H₂₉BF₂₄IOP: C, 47.77; H, 2.28. Found: C, 47.86; H, 2.40. **¹H NMR** (400 MHz, DCM, 18.9 °C): δ = 7.85 (t, *J* = 7.3, 7.8 Hz, 1H, *Ph*), 7.79 (t, *J* = 7.8 Hz, 2H, *Ph*), 7.71 (s, 8H, Ar*H* (BAr^F)), 7.66 (q, *J* = 5.0, 7.3, 8.2 Hz, 4H, *Ph*), 7.58 (dd, *J* = 7.3, 16.5 Hz, 4H, *Ph*), 7.54 (s, 4H, Ar*H* (BAr^F)), 7.17 (q, *J* = 7.8 Hz, 2H, *Ph*), 6.93 (dd, *J* = 7.8, 16.5 Hz, 1H, *Ph*), 3.8 (s, 3H, O*Me*). **³¹P NMR** (161.8 MHz, DCM, 18.9 °C): δ = 2.6 (s). **¹³C{¹H} NMR** (100.5 MHz, DCM, 19.0°C): δ = 162.3 (d, J_{C-P} = 1.9 Hz, *Ph*), 161.9 (q, J_{C-B} = 49.8 Hz, aromatic *C* (BAr^F)), 140.0 (d, J_{C-P} 2.9

Hz, *Ph*), 136.3 (d, J_{C-P} = 2.9 Hz, *Ph*), 135.6 (d, J_{C-P} = 9.6 Hz, *Ph*), 134.9 (bs, aromatic *C* (BAr^F)), 133.5 (d, J_{C-P} = 12.5 Hz, *Ph*), 130.5 (d, J_{C-P} = 14.4 Hz, *Ph*), 129.0 (qq, J_{C-F} = 31.6 Hz, J_{C-B} = 2.9 Hz, *C*-CF$_3$ (BAr^F)), 124.7 (q, J_{C-F} = 272.2, 272.7 Hz, *CF$_3$* (BAr^F)), 122.5 (d, J_{C-P} = 14.4 Hz, *Ph*), 119.9 (d, J_{C-P} = 82.4 Hz, *Ph*), 117.6 (m, aromatic *C* (BAr^F)), 113.5 (d, J_{C-P} = 6.7 Hz, *Ph*), 56.5 (s, O*Me*). **^{11}B NMR** (128.3 MHz, DCM, 18.6 °C): δ = -8.2 (s, *B*Ar^F). **^{19}F NMR** (376.2 MHz, DCM, 18.4 °C): δ = -63.3 (s, C*F$_3$* (BAr^F)). **SCXRD** P-1, a 12.3441(3) Å, b 13.0277(2) Å, c 19.3179(3) Å, α 86.9054(14) °, β 82.8373(15) °, γ 71.4746(17) °, R$_1$/wR$_2$ 0.0541/ 0.1378.

Synthesis of [Ph$_2$P(*o*-NMe$_2$-C$_6$H$_4$)I][BAr^F] [3b]BAr^F: (pale yellow solid, 69% yield). Despite repeat syntheses and recrystallisations, we were unable to isolate the product free of phosphine oxide impurity (less than 5% by NMR). *Anal.* Calc. for C$_{52}$H$_{32}$BF$_{24}$INP: C, 48.21; H, 2.49; N, 1.08. Found: C, 48.15: H, 2.40; N, 1.15. **^{1}H NMR** (400 MHz, DCM, 17.0 °C): δ = 7.96-7.89 (m, 1H, *Ph*), 7.78-7.73 (br, 2H, *Ph*), 7.72 (br, 8H, Ar*H* (BAr^F)), 7.69-7.63 (m, 6H, *Ph*), 7.62-7.55 (m, 5H, *Ph*), 7.54 (br, 4H, Ar*H* (BAr^F)), 2.12 (s, 6H, N*Me$_2$*). **^{31}P NMR** (161.8 MHz, DCM, 17.6 °C): δ = 6.1 (s). **^{13}C{^{1}H} NMR** (100.5 MHz, DCM, 16.8 °C): δ = 161.2 (q, J_{C-B} = 49.8 Hz, aromatic *C* (BAr^F)), 159.4 (d, J_{C-P} = 5.8 Hz, *Ph*), 139.4 (d, J_{C-P} = 2.4 Hz, *Ph*), 136.7 (d, J_{C-P} = 12.5 Hz, *Ph*), 135.7 (d, J_{C-P} = 3.4 Hz, *Ph*), 134.9 (br, aromatic *C* (BAr^F)), 133.0 (d, J_{C-P} = 12.0 Hz, *Ph*), 130.4 (d, J_{C-P} = 14.89 Hz, *Ph*), 129.0 (qq, J_{C-F} = 31.6 Hz, J_{C-B} = 2.9 Hz, *C*-CF$_3$ (BAr^F)), 127.3 (d, $J_{C=P}$ = 8.2 Hz, *Ph*), 124.7 (q, J_{C-F} = 272.2, 272.7 Hz, *CF$_3$* (BAr^F)), 122.1 (d, J_{C-P} = 82.9 Hz, *Ph*), 118.6 (d, J_{C-P} = 88.2 Hz, *Ph*), 117.6 (m, aromatic *C* (BAr^F)), 45.6 (s, N*Me$_2$*). **^{11}B NMR** (128.3 MHz, DCM, 17.2°C): δ = -8.2 (s, *B*Ar^F). **^{19}F NMR** (376.2 MHz, DCM, 17.4 °C): δ = -63.3 (s, C*F$_3$* (BAr^F)). **SCXRD** P-1, a 12.50066(15) Å, b 13.24451(17) Å, c 17.59462(19) Å, α 90.5505(10) °, β 92.5441(9) °, γ 109.5891(12) °, R$_1$/wR$_2$ 0.0313/ 0.0826.

Synthesis of [PhP(*o*-OMe-C$_6$H$_4$)$_2$I][BAr^F] [3d]BAr^F: (colourless solid, 46% yield). *Anal*. Calc. for C$_{52}$H$_{31}$BF$_{24}$IO$_2$P: C, 47.59; H, 2.38. Found: C, 47.40; H, 2.30. **^{1}H NMR** (400 MHz, DCM, 17.2 °C): δ = 7.82 (t, *J* = 7.4, 8.0 Hz, 2H, *Ph*), 7.76 (br, 1H, *Ph*), 7.71 (br, 8H, Ar*H* (BAr^F)), 7.67-7.57 (m, 4H, *Ph*), 7.54 (br, 4H, Ar*H* (BAr^F)), 7.15 (q, *J* = 7.3, 8.0 Hz, 4H, *Ph*), 7.01 (dd, *J* = 7.6, 17.3 Hz, 2H, *Ph*), 3.81 (s, 6H, O*Me*). **^{31}P NMR** (161.8 MHz, DCM, 16.7 °C): δ = -10.0 (s). **^{13}C{^{1}H} NMR** (100.5 MHz, DCM, 17.5 °C): δ = 162.1 (d, $J_{C\text{-}P}$ = 2.9 Hz, *Ph*), 161.9 (q, $J_{C\text{-}B}$ = 49.8 Hz, aromatic *C* (BAr^F)), 139.2 (d, $J_{C\text{-}P}$ = 1.9 Hz, *Ph*), 135.7 (d, $J_{C\text{-}P}$ = 3.4 Hz, *Ph*), 135.1 (d, $J_{C\text{-}P}$ = 10.1 Hz, *Ph*), 134.9 (br, aromatic *C* (BAr^F)), 133.2 (d, $J_{C\text{-}P}$ = 12.0 Hz, *Ph*), 130.2 (d, $J_{C\text{-}P}$ = 14.9 Hz, *Ph*), 129.0 (qq, $J_{C\text{-}F}$ = 31.6 Hz, $J_{C\text{-}B}$ = 2.9 Hz, *C*-CF$_3$ (BAr^F)), 124.7 (q, $J_{C\text{-}F}$ = 272.2, 272.7 Hz, CF$_3$ (BAr^F)), 122.2 (d, $J_{C\text{-}P}$ = 14.4 Hz, *Ph*), 120.1 (d, $J_{C\text{-}P}$ = 85.8 Hz, *Ph*), 117.6 (m, aromatic *C* (BAr^F)), 113.3 (d, $J_{C\text{-}P}$ = 6.7 Hz. *Ph*), 105.8 (d, $J_{C\text{-}P}$ = 85.8 Hz, *Ph*), 56.3 (s, O*Me*).). **^{11}B NMR** (128.3 MHz, DCM, 17.3 °C): δ = -8.2 (s, *B*Ar^F). **^{19}F NMR** (376.2 MHz, DCM, 17.3 °C): δ = -63.3 (s, C*F$_3$* (BAr^F)). **SCXRD** P2$_1$, a 12.46086(15) Å, b 34.0625(3) Å, c 13.54015(16) Å, α 90°, β 110.6112(13) °, γ 90 °, R$_1$/wR$_2$ 0.0354/0.0887.

Synthesis of [PhP(*o*-NMe$_2$-C$_6$H$_4$)$_2$I][BAr^F] [3e]BAr^F: (pale orange solid, 49% yield). Slow diffusion of hexane into a saturated solution of the product in DCM afforded an orange oil and no crystals suitable for X-ray diffraction. *Anal.* Calc. for C$_{55}$H$_{37}$BF$_{24}$IN$_2$P: C, 48.45; H, 2.79; N, 2.09. Found: C, 48.39; H, 2.72; N, 2.12. **^{1}H NMR** (400 MHz, DCM, 17.1 °C): δ = 7.96 (dd, *J* = 8.0, 16.4 Hz, 2H, *Ph*), 7.86 (t, *J* = 7.7 Hz, 2H, *Ph*), 7.71 (br, 8H, Ar*H* (BAr^F)), 7.67-7.57 (m, 5H, *Ph*), 7.54 (br, 4H, Ar*H* (BAr^F)), 7.50 (t, *J* = 7.7, 7.9 Hz, 4H, *Ph*), 2.07 (s, 12H, N*Me$_2$*). **^{31}P NMR** (161.8 MHz, DCM, 17.0 °C): δ = -3.0 (s). **^{13}C{^{1}H} NMR** (100.5 MHz, DCM, 18.5 °C): δ = 161.9 (q, $J_{C\text{-}B}$ = 49.8 Hz, aromatic *C* (BAr^F)), 158.6 (d, $J_{C\text{-}P}$ = 5.3 Hz, *Ph*), 138.0 (d, $J_{C\text{-}P}$ = 2.4 Hz, *Ph*), 134.9 (br, aromatic *C* (BAr^F)), 131.4 (d, $J_{C\text{-}P}$ = 11.5 Hz, *Ph*), 129.8 (d, $J_{C\text{-}P}$ = 14.4 Hz,

Ph), 129.0 (qq, J_{C-F} = 31.6 Hz, J_{C-B} = 2.9 Hz, *C*-CF$_3$ (BAr^F)), 126.6 (d, J_{C-P} = 8.6 Hz, *Ph*), 126.3 (d, J_{C-P} = 85.3 Hz, *Ph*), 124.7 (q, J_{C-F} = 272.2, 272.7 Hz, CF$_3$ (BAr^F)), 117.6 (m, aromatic *C* (BAr^F)), 45.75 (s, N*Me$_2$*). **^{11}B NMR** (128.3 MHz, DCM, 18.1 °C): δ = -8.2 (s, *B*Ar^F). **^{19}F NMR** (376.2 MHz, DCM, 17.7 °C): δ = -63.3 (s, C*F$_3$* (BAr^F)).

Synthesis of [PPh$_3$I][BAr^F] [3g]BAr^F: (colourless solid, 75% yield). *Anal.* Calc. for C$_{50}$H$_{27}$BF$_{24}$IP: C, 47.95; H, 2.17. Found: C, 48.03; H, 2.03. **^{1}H NMR** (400 MHz, DCM, 16.9 °C): δ = 7.83 (t, *J* = 7.3, 7.8 Hz, 3H, *Ph* (PPh$_3$I)), 7.75-7.66 (m, 14H, *Ph,* Ar*H* (PPh$_3$I, BAr^F)), 7.59 (dd, *J* = 8.0, 15.8 Hz, 6H, *Ph* (PPh$_3$I)), 7.54 (s, 4H, Ar*H* (BAr^F)). **^{31}P NMR** (161.8 MHz, DCM, 17.1°C): δ = 14.1 (s). **^{13}C{^{1}H} NMR** (100.5 MHz, DCM, 18.1 °C): δ = 161.9 (q, J_{C-B} = 49.8 Hz, aromatic *C* (BAr^F)), 137.0 (d, J_{C-P} = 3.8 Hz, *Ph*), 134.9 (bs, aromatic *C* (BAr^F)), 134.0 (d, J_{C-P} = 12.5 Hz, *Ph*), 130.9 (d, J_{C-P} = 14.9 Hz, *Ph*), 123.0 (qq, J_{C-F} = 31.6 Hz, J_{C-B} = 2.9 Hz, *C*-CF$_3$ (BAr^F)), 124.7 (q, J_{C-F} = 272.2, 272.7 Hz, CF$_3$ (BAr^F)), 119.7 (d, J_{C-P} = 79.1 Hz, *Ph*), 117.6 (m, aromatic *C* (BAr^F)). **^{11}B NMR** (128.3 MHz, DCM, 17.0 °C): δ = -8.2 (s, *B*Ar^F). **^{19}F NMR** (376.2 MHz, DCM, 17.7 °C): δ = -63.3 (s, C*F$_3$* (BAr^F)). **SCXRD** P-1, a 12.47595(15) Å, b 13.15500(16) Å, c 17.7202(2) Å, α 90.8265(10) °, β 110.2111(11) °, γ 109.0350(11) °, R$_1$/wR$_2$ 0.0385/ 0.0950.

Synthesis of [Ph$_2$P(*o*-OMe-C$_6$H$_4$)I][I$_3$] [3a]I$_3$: (dark red solid, 54% yield). *Anal.* Calc. for C$_{19}$H$_{17}$I$_4$OP: C, 28.53; H, 2.14. Found: C, 28.61; H, 2.00. **^{1}H NMR** (400 MHz, DCM, 18.1 °C): δ = 7.88 (t, *J* = 7.3, 7.6 Hz, 1H, *Ph*), 7.84-7.77 (m, 2H, *Ph*), 7.73-7.65 (m, 5H, *Ph*), 7.62 (t, *J* = 7.6, 8.0 Hz, 3H, *Ph*), 7.26-7.15 (m, 2H, *Ph*), 6.98 (dd, *J* = 7.8, 16.3 Hz, 1H, *Ph*), 3.87 (s, 3H, O*Me*). **^{31}P NMR** (161.8 MHz, DCM, 18.4 °C): δ = -2.4 (s). **^{13}C{^{1}H} NMR** (100.5 MHz, DCM, 18.6 °C): δ = 162.2 (d, J_{C-P} = 2.4 Hz, *Ph*), 139.4 (d, J_{C-P} = 2.4 Hz, *Ph*), 135.7 (d, J_{C-P} = 3.4 Hz, *Ph*), 135.5 (d, J_{C-P} = 9.6 Hz, *Ph*), 133.7 (d, J_{C-P} = 11.5 Hz, *Ph*), 130.4 (d, J_{C-P} = 14.4 Hz, *Ph*), 122.4

(d, J_{C-P} = 13.9 Hz, *Ph*), 120.7 (d, J_{C-P} = 78.6 Hz, *Ph*), 113.5 (d, J_{C-P} = 6.7 Hz, *Ph*), 106.7 (d, J_{C-P} = 79.1 Hz, *Ph*), 56.9 (s, O*Me*).

Synthesis of [PhP(*o*-OMe-C$_6$H$_4$)$_2$I][I$_3$] [3d]I$_3$: (dark orange solid, 66% yield). *Anal.* Calc. for C$_{20}$H$_{19}$I$_4$O$_2$P: C, 28.94; H, 2.31. Found: C, 28.85; H, 2.25. **^{1}H NMR** (400 MHz, DCM, 17.2 °C): δ = 7.85 (t, *J* = 7.1, 7.3 Hz, 2H, *Ph*), 7.77 (t, *J* = 7.1 Hz, 1H, *Ph*), 7.70-7.59 (m, 4H, *Ph*), 7.20 (q, *J* = 7.6, 8.2 Hz, 4H, *Ph*), 7.06 (dd, *J* = 7.8, 16.9 Hz, 2H, *Ph*), 3.85 (s, 6H, O*Me*). **^{31}P NMR** (161.8 MHz, DCM, 17.3 °C): δ = -13.0 (s). **^{13}C{^{1}H} NMR** (100.5 MHz, DCM, 17.2 °C): δ = 162.0 (d, J_{C-P} = 2.4 Hz, *Ph*), 138.8 (d, J_{C-P} = 2.4 Hz, *Ph*), 135.3 (d, J_{C-P} = 3.4 Hz, *Ph*), 135.2 (d, J_{C-P} = 9.6 Hz, *Ph*), 133.4 (d, J_{C-P} = 12.0 Hz, *Ph*), 130.1 (d, J_{C-P} = 14.4 Hz, *Ph*), 122.2 (d, J_{C-P} = 14.4 Hz, *Ph*), 120.7 (d, J_{C-P} = 82.4 Hz, *Ph*), 113.4 (d, J_{C-P} = 7.2 Hz, *Ph*), 106.5 (d, J_{C-P} = 82.9 Hz, *Ph*), 56.7 (s, O*Me*). **SCXRD** P2$_1$/n, a 14.5165(2) Å, b 17.6860(3) Å, c 22.1653(4) Å, α 90 °, β 103.2846(17) °, γ 90 °, R$_1$/wR$_2$ 0.0300/0.0810.

Synthesis of [PhP(*o*-NMe$_2$-C$_6$H$_4$)$_2$I][I$_3$] [3e]I$_3$: (dark red solid, 72% yield). *Anal.* Calc. for C$_{22}$H$_{25}$I$_4$N$_2$P: C, 30.87; H, 2.94; N, 3.27. Found: C, 30.69; H, 2.85; N, 3.26. **^{1}H NMR** (400 MHz, DCM, 17.0 °C): δ = 8.0 (dd, *J* = 7.8, 16.5 Hz, 2H, *Ph*), 7.90 (t, *J* = 7.3, 7.8 Hz, 2H, *Ph*), 7.75-7.63 (m, 5H, *Ph*), 7.59 (dd, *J* = 7.8, 15.1 Hz, 2H, *Ph*), 7.55 (t, *J* = 7.3, 7.8 Hz, 2H, *Ph*), 2.12 (s, 12H, N*Me$_2$*). **^{31}P NMR** (161.8 MHz, DCM, 17.8 °C): δ = -5.3 (s). **^{13}C{^{1}H} NMR** (100.5 MHz, DCM, 17.6 °C): δ = 158.6 (d, J_{C-P} = 5.8 Hz, *Ph*), 137.6 (d, J_{C-P} = 2.4 Hz, *Ph*), 135.6 (br, *Ph*), 134.6 (d, J_{C-P} = 3.8 Hz, *Ph*), 131.5 (d, J_{C-P} = 11.5 Hz, *Ph*), 129.8 (d, J_{C-P} = 14.4 Hz, *Ph*), 128.5 (d, J_{C-P} = 14.9 Hz, *Ph*), 126.5 (d, J_{C-P} = 8.6 Hz, *Ph*), 126.4 (d, J_{C-P} = 82.9 Hz, *Ph*), 120.0 (d, J_{C-P} = 92.0 Hz, *Ph*), 45.9 (s, N*Me$_2$*). **SCXRD**

P2$_1$/n, a 11.9475(3) Å, b 16.4754(4) Å, c 13.5533(3) Å, α 90 °, β 98.650(2) °, γ 90 °, R$_1$/wR$_2$ 0.0211/ 0.0412.

Synthesis of [PPh$_3$I][I$_3$] [3g]I$_3$: PPh$_3$ (0.100 g, 0.381 mmol) was dissolved in Et$_2$O (10cm^3) and iodine (0.194g, 0.762 mmol) was added dropwise as a solution in Et$_2$O (10cm^3), forming a bright yellow precipitate which darkened as addition continued. After stirring overnight, the supernatant was removed *via* filtration and the solids were washed with Et$_2$O (2 x 5 cm^3) then dried *in vacuo* yielding the product as a free flowing dark red powder (0.262 g, 0.340 mmol, 89% yield). Single crystals suitable for X-ray diffraction were grown by slow diffusion of diethyl ether into a concentrated solution of the product in DCM. *Anal.* Calc. for C$_{18}$H$_{15}$PI$_4$: C, 28.08; H, 1.96. Found: C, 28.16; H, 1.87. **^{1}H NMR** (400 MHz, DCM, 18.6 °C): δ = 7.84 (td, *J* = 2.5, 7.1, 7.8 Hz, 3H, *Ph*), 7.72 (sex, *J* = 3.0, 3.7, 4.4, 4.6 Hz, 6H, *Ph*), 7.64 (dd, *J* = 7.6, 15.3 Hz, 6H, *Ph*). **^{31}P NMR** (161.8 MHz, DCM, 18.1 °C): δ = 6.0 (s). **^{13}C{^{1}H} NMR** (100.5 MHz, DCM, 18.5 °C): δ = 136.1 (d, *J$_{C-P}$* = 2.9 Hz, *Ph*), 133.9 (d, *J$_{C-P}$* = 11.5 Hz, *Ph*), 130.7 (d, *J$_{C-P}$* = 14.4 Hz, *Ph*), 120.6 (d, *J$_{C-P}$* = 74.8 Hz, *Ph*). **SCXRD** Pnma, a 12.2921(3) Å, b 38.2596(10) Å, c 9.0269(2) Å, α 90 °, β 90 °, γ 90 °, R$_1$/wR$_2$ 0.0395/0.0734.

Crystal Data for [4]I$_3$: **SCXRD** P2$_1$2$_1$2$_1$, a 18.3990(2) Å, b 12.17869(14) Å, c 9.99371(12) Å, α 90 °, β 90 °, γ 90 °, R$_1$/wR$_2$ 0.0253/0.0703.

Results and Discussion

Synthesis and Structure of Ar$_3$PI$_2$ Adducts

The diiodophosphoranes were readily prepared by the reaction of equimolar donor-functionalised phosphane and diiodine in dry diethyl ether under dry argon. Crystals of the diiodide adducts suitable for diffraction studies were obtained *via* slow diffusion of

diethyl ether into a saturated solution of the product in dichloromethane. We were unable to isolate phosphane **1f** (D=CH$_2$NMe$_2$, D'=CH$_2$NMe$_2$) without residual phosphine oxide impurity which was found to interfere with subsequent reactions. In light of this and the observed rearrangements of [**3d**]I$_3$ to [**4**]I$_3$, (*vide infra*) no further studies were made using this ligand.

The five new adducts structurally characterised show the expected charge-transfer "spoke" motif in the solid state, and the ^{31}P NMR data, as seen in Table 1, are upfield shifted with respect to **2g** and indicate that this structure is maintained in solution in DCM.[25] The P-I-I angles are close to linear, ranging from 171.02(3)° for **2e** to 178.27(2)° for **2a**. P-I and I-I distances fall well within the large range observed for other R$_3$PI$_2$ adducts but generally have slightly longer I-I bond lengths in comparison to other Ar$_3$PI$_2$ adducts as a result of greater electron donating capacity.

	Bond Lengths / Å				Bond Angles / °			
	P-I	I-I	D-P	D'-P	D-P-C	D'-P-C	D'-P-I	δ [31]P
2a	2.4753(6)	3.2022(3)	2.910(2)		159.2(1)			-23.4
2b	2.4913(5)	3.1238(3)	2.898(1)		161.89(7)			-25.8
2c	2.4791(7)	3.1884(3)	2.951(3)		177.8(1)			-23.1
2d	2.4610(6)	3.2648(3)	2.896(2)	2.898(1)	160.27(1)	162.93(7)		-31.1
2e	2.4377(9)	3.3502(4)	2.883(3)	2.945(3)	165.3(1)		167.95(6)	-22.7
	2.4622(7)	3.2464(4)	2.904(3)	2.933(2)	166.7(1)		169.21(6)	
2g	2.4690(8)	3.1513(3)						-19.8

Table 1: Selected crystallographic bond lengths and angles for diiodophosphoranes, and ^{31}P NMR chemical shifts. D is the donor centre involved in the primary donor-phosphorus-phenyl hypervalent bonding mode; D' is the donor centre involved in the secondary hypervalent contact.

Oxygen-donor compounds **2a** and **2d** both crystallise with a single molecule in their asymmetric units (Figure 1) in geometries intermediate between tetrahedral and trigonal bipyramidal, with apical methoxy and phenyl substituents. The phosphorus-iodine bond of **2a** is comparable to that of **2g** (2.4753(6) *vs* 2.4690(8) Å), whilst that of **2d** is considerably shorter at 2.4610(6) Å, but the iodine-iodine bond is elongated in both cases (**2a**: 3.2022(3) and **2d**: 3.2648(3) Å *vs* **2g**: 3.1513(3) Å, *cf.* 2.660 Å for I$_2$).[29] The methoxy groups are coplanar with the associated benzene rings in all cases, and show apparent close contacts between the oxygen and phosphorus centres (dO(1)-P(1) **2a**: 2.910(2) Å, **2d**: 2.896(2) Å and 2.898(1) Å), within the sum of the van der Waals radii (3.32 Å), leading to apparent distorted pentacoordinate and hexacoordinate structures. However, the C$_{Ar}$-O bonds are short (**2a**: 1.357(3) Å, **2d**: 1.354(2) Å and 1.358(3) Å) compared to that of free anisole (1.372(1) Å)[50], indicating a more significant degree of delocalisation of the oxygen lone pairs onto the ring. The O-P-C$_{apical}$ angles deviates considerably from linearity, (**2a**: 159.2(1)°, **2d**: 160.24(7)° and 162.93(7)°) and the structure is therefore better described as possessing a tetrahedral phosphorus environment with the increased donor strength of the phosphanes (as demonstrated by the increased I-I distances) arising from π-conjugation of the oxygen lone pairs rather than hypervalent bond formation - the close O-P contacts must therefore arise of steric necessity.
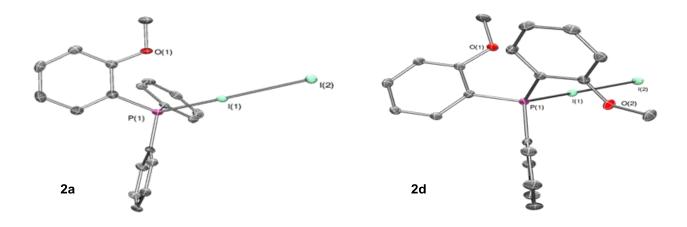
Figure 1: Molecular structures of **2a** and **2d**. Drawn with ellipsoids at 50% probability; hydrogens omitted for clarity.

Compounds **2b** likewise crystallises with a single molecule in the asymmetric unit, whilst **2e** crystallises with two symmetry inequivalent molecules in the asymmetric unit (Figure 2). Close contacts are seen between the pendant nitrogens and the phosphorus centres (**2b**: dN(1)-P(1) = 2.898(1) Å, **2e**: molecule 1, dN(1)-P(1) = 2.883(3) Å, dN(2)-P(1) = 2.945(3) Å; molecule 2, dN(3)-P(2) = 2.904(3) Å, dN(4)-P(2) = 2.933(2) Å), shorter than the sum of the van der Waals radii (3.32 Å), but considerably longer than typical P-N single bonds (1.730 Å).[51] Unlike **2a**, the donor NMe_2 fragments are rotated such that the lone pairs are orthogonal to the π-system, and directed towards the donor phosphorus centre. In **2e**, contrary to **2d**, only one donor-phosphorus interaction is apparently *trans* to an apical arene ring, and the second donor now occupies a position *trans* to the iodine spoke. The N-P-X angles still deviates significantly from linearity (**2b**: 161.89(7)°, **2e**: 165.3(1)° to 169.21(6)°), likely due to the rigidity of the chelate tether but less so than for **2a** and **2d**. Interestingly, for **2b** the P-I bond is, at 2.4913(5) Å, significantly longer than that of **2g**,

whilst the I-I distance is considerably shorter at 3.1238(3) Å and thus despite the donation of the lone pair onto phosphorus, the contraction of the I-I bond indicates that the overall degree of charge transfer is in fact less than that of **2g**. In contrast, **2e** shows significant contraction of the P-I bonds (2.4377(9) Å and 2.4622(7) Å) and elongation of the I-I bonds (3.3502(4) Å and 3.2464(4) Å) relative to **2g**. The significant difference seen in I-I contacts between the two molecules shows that packing effects and interactions are significant in these systems, though it must be noted that this is seen for the most electron-rich phosphorus centre and thus the weakest and most-labile I-I bonds. The P-I bond contraction occurs despite the significant increase in steric hindrance expected in going from penta- to hexa-coordination, supporting the presence of true and significant hypervalency (and confirmed through computational modelling, *vide infra*), confirming that **2e** is thus the first neutral hexacoordinate P(III) complex to our knowledge.
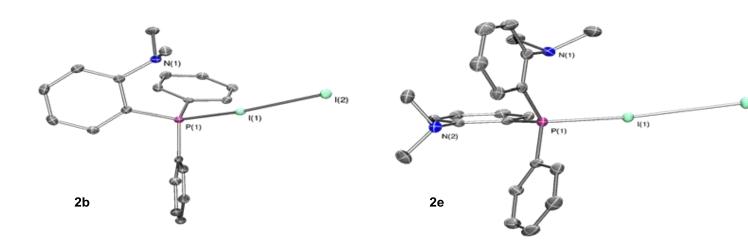

2b   2e

Figure 2: Molecular structure of **2b** and **2e**. Drawn with ellipsoids at 50% probability; hydrogens omitted for clarity.

Compound **2c** (Figure 3) crystallises as an unambiguous pentacoordinate phosphorus species with a single molecule in the asymmetric unit – the sum of angles about the equatorial plane is 339.7° and the nitrogen-phosphorus contact is 2.951(3) Å, slightly longer than that of **2b** but within the sum of the van der Waals radii. This molecule is sufficiently flexible, due to the methylene linker, to twist the NMe_2 group away to minimise steric clashes, but nevertheless adopts an apical position, linearly *trans* to a phenyl group – the N-P-C*apical* angle is 177.8(1)°. The P-I bond length (2.4791(7) Å) is again comparable to **2g**, but the I-I bond (3.1884(3) Å) is elongated, indicating a greater degree of charge transfer.
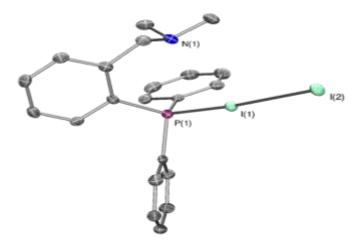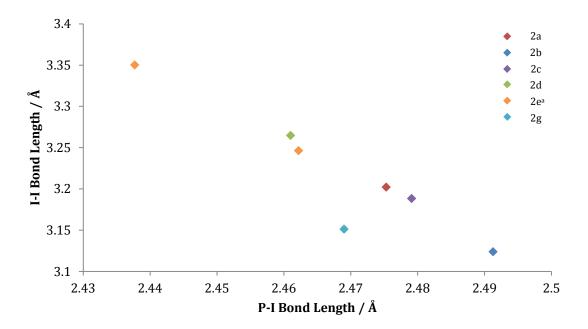

Figure 3: Molecular structure of **2c**. Drawn with ellipsoids at 50% probability; hydrogens omitted for clarity.

Comparison of the bonding between the diiodophosphoranes within the internally solvated set and **2g** (see Table 1) allows the relative "phosphorus donor strength" to be determined taking into account combined electronic and steric effects. An inverse, linear relationship between P-I bond length and I-I bond length is observed and shown in Graph 1 with the I-I distances showing a much greater variation in length. From the variation in I-I bond lengths, we can see that of the singly substituted phosphanes, **1a** is the strongest donor, followed by **1c** and then **1b**. However, the P-I bond is essentially invariant within errors for **2a** and **2d** compared to **2g** and so the steric demand must be significant even for a single additional substituent.

Graph 1: I-I bond lengths *vs* P-I bond lengths for the donor-functionalised diiodophosphoranes. [a] Compound **2e** crystallises with two metrically dissimilar molecules in the asymmetric unit and both are indicated here.

Upon the addition of a second donor group with **1d** and **1e**, there is a decrease in P-I bond lengths despite the increased steric demand of the more congested phosphorus centre and an increase in I-I distances indicating a much greater degree of charge transfer.

21

Gratifyingly, **2b** and **2c** both show N-P-C *3c4e⁻* bonding interactions in preference to the potential N-P-I motif – it is only for **2e** that both become observed – this supports the existence of hypervalent bonding in these systems, which is stabilised by electronegative apical moieties. That the additional donor capacity of **1a** and **1d** arises from conjugation through the aromatic systems is further supported by examination of the known structure for tris(2,4,6-trimethoxyphenyl)diiodophosphorane,[52] which shows greater P-I separation (2.482(1) Å) than **2e** but comparable I-I distances (3.3394(5) Å) and no evidence of any O-P-I alignment, with all methoxy fragments essentially coplanar with the aromatic rings – the additional potential donor strength is therefore significantly offset by the increased steric bulk of the additional *ortho*-substituents.[25]

Synthesis and Structure of Iodophosphonium Salts

Combination of donor-functionalised diiodophosphoranes **2a-2e** with NaBAr^F or I_2 in dichloromethane yielded the corresponding iodophosphonium salts, as seen by an immediate downfield shift in the ^{31}P NMR spectra. As with PPh$_3$ and I_2,[53] there is a smooth shift to higher chemical shifts when NaBAr^F or I_2 are added and discrete starting material and product peaks are not observed. There is also a noticeable shift in the ^1H NMR spectra for the donor moieties: a downfield shift when D = OMe (**3a** and **3d**); and an upfield shift when D = NMe$_2$ or CH$_2$NMe$_2$ (**3b**, **3c**, and **3e**), although this shift is insignificant compared to the changes in the ^{31}P NMR. The known compound **[3g]**I$_3$ was prepared and single-crystal X-ray diffraction data was collected at 100K to allow comparison of data sets collected under equivalent conditions. Slow diffusion of diethyl ether into a saturated solution of [**3g**][I$_3$] in dichloromethane provided single crystals of the [(Ph$_3$PI)$_2$I$_3$]I$_3$ polymorph[54] suitable for diffraction studies; the diffraction data of this known compound were recollected and solved to provide datasets collected at equivalent temperatures to allow dataset comparisons.

	Bond Lengths / Å				Bond Angles / °			δ ^{31}P
	P-I	D-P	D'-P	I(1)-I$_3$	D-P-C	D'-P-C	D'-P-I	
[3a]BAr^F	2.376(1)	2.855(5)			164.3(2)			2.6
[3b]BAr^F	2.3792(6)	2.920(3)			164.8(1)			6.1
[3d]BAr^F	2.385(1)	2.875(5)	2.898(4)		163.2(2)	161.9(2)		-10.0
	2.382(1)	2.877(5)	2.902(3)		163.4(2)	161.4(2)		
[3g]BAr^F	2.3795(6)							14.1
[3d]I$_3$	2.407(1)	2.895(3)	2.901(3)	3.5167(5)	161.8(2)	163.1(2)		-13.0
	2.411(1)	2.870(3)	2.886(3)	3.4872(5)	163.0(1)	163.5(2)		
[3e]I$_3$	2.427(1)	2.892(3)	2.845(3)	3.5802(4)	166.7(1)		167.86(6)	-5.3
[3g]I$_3$	2.408(2)			3.4837(2)				-6.0

Table 2: Selected crystallographic bond lengths and angles for iodophosphonium cations, and ^{31}P NMR chemical shifts. D is the donor centre involved in the primary donor-phosphorus-phenyl hypervalent bonding mode; D' is the donor centre involved in the secondary hypervalent contact.

For the seven crystallographically characterised iodophosphonium salts, there is, unsurprisingly, significant structural similarity between the ionic salts and the corresponding parent diiodophosphoranes (Figure 4). The **3** salts are well separated ion pairs, and both [**3d**]BAr^F and [**3d**]I$_3$ crystallise with two ionic inequivalent subunits in the asymmetric unit. In all cases, the P-I bond length is significantly contracted in comparison to the Ar$_3$PI$_2$ adducts, with the BAr^F salts having slightly shorter P-I distances than the triiodide salts as seen in Table 2. Polymorphism is commonly observed in R$_3$PI$_4$ systems, with structural differences arising from different association modes between the terminal iodide of the phosphonium cation and the triiodide

23

anion.[55] As might be expected by the facility with which iodine species undergo concatenation, these contacts are weakly covalent and so affect overall P-I bonding.
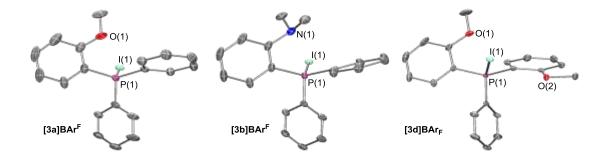

Figure 4: Cationic structures of [**3a**]BAr^F, [**3b**]BAr^F and [**3d**]BAr^F. Drawn with ellipsoids at 30% probability, hydrogen atoms, disordered counterion and solvents of crystallisation omitted for clarity. Only one of the two symmetry inequivalent cations of [**3d**]BAr^F is shown.

The P-I bond lengths for [**3a**]BAr^F, [**3b**]BAr^F and [**3g**]BAr^F are all equivalent within errors [2.376(1) Å, 2.3792(6) Å and 2.3795(6) Å respectively] whereas the P-I distances in **2a**, **2b** and **2g** are significantly different [2.4753(6) Å, 2.4913(5) Å and 2.4690(8) Å respectively]. On the other hand, the P-I distance in [**3d**]BAr^F (molecule 1, d(P-I) = 2.382(1) Å; molecule 2, d(P-I)= 2.385(1) Å) is larger than those of the other structurally characterised BAr^F salts despite the P-I bond length for **2d** (2.4610(6) Å) being significantly shorter than that observed in **2a**, **2b** and **2g**. This is attributed to the increased steric demand at the phosphorus centre caused by having two *ortho*-substituents. For [**3a**]BAr^F, the C_{Ar}-O(1) distance (1.344(7) Å) contracts relative to **2a** to accommodate for the shorter P-I bond length and increased steric demand at the phosphorus centre. The O(1)-C_{Ar}-C_P angles remains identical but the C_{Ar}-C_P-P angle decreases slightly

resulting in a reduced O(1)-P(1) contact (2.855(5) Å) relative to **2a**. In contrast, for [**3b**]BAr^F, the C$_{Ar}$-N(1) distance remains unchanged whilst the N(1)-C$_{Ar}$-C$_P$ and C$_{Ar}$-C$_P$-P angles increase comparative to **2b** resulting in an elongated N(1)-P(1) contact (2.920(3) Å *vs*. 2.898(1) Å for **2b**). Upon addition of a second donor to give [**3d**]BAr^F, the dO(1)-P contact shortens slightly relative to **2d** (molecule 1, 2.875(5) Å; molecule 2, 2.877(5) Å *vs*. 2.896(2) Å) whilst the dO(2)-P distances are maintained. Unlike [**3a**]BAr^F and [**3b**]BAr^F, the C$_{Ar}$-O(1) distance and the O(1)-C$_{Ar}$-C$_P$ angle remain constant whilst the C$_P$-P(1) bond length contracts very slightly (molecule 1, 1.782(5) Å; molecule 2, 1.780(5) Å *vs*. 1.790(5) Å for [**3a**]BAr^F and 1.792(2) Å for [**3b**]BAr^F), resulting in a reduced oxygen-phosphorus contact. The C$_{Ar}$-O distances in in [**3a**]BAr^F and [**3d**]BAr^F are short ([**3a**]BAr^F, 1.344(7) Å, [**3d**]BAr^F 1.337(6) Å to 1.356(7) Å) but these distances remains longer than a typical carbon-oxygen double bond (1.2183 Å for benzoquinone)[56] or a carbon-oxygen single bond that has substantial double bond character (1.2813 Å for benzoic acid at 100 K)[57] but confirm significant π-conjugation of the oxygen lone pairs into the arene ring.

No trends in apparent donor strength can be established for the triiodide salts since only two of the donor-functionalised iodophosphonium triiodides were structurally characterised (Figure 5). Unlike [**3d**]BAr^F, the P-I bond length in [**3d**]I$_3$ is essentially identical to [**3g**]I$_3$ (molecule 1, d(P-I) = 2.407(1) Å; molecule 2, d(P-I)= 2.411(1) Å *vs*. d(P-I) = 2.408(2) Å), whereas the P-I bond length in [**3e**]I$_3$ is significantly elongated (2.427(1) Å). However, the P-I distance for **2e** is the shortest observed for the donor-functionalised diiodophosphoranes and contracts to a much lesser degree upon forming the corresponding triiodide as compared to **2d** and **2g**. Again, the long P-I bond length in [**3e**]I$_3$ is believed to arise from the increased steric demand at phosphorus due to the two *ortho*-substituents.

Compound [**3d**]I₃ crystallises with two molecules in the asymmetric unit, both adopting similar structures and bond metrics. In fact, the O-P distances, C$_{Ar}$-O and C$_P$-P bond lengths, and the O-C$_{Ar}$-C$_P$ angles are identical within errors for the two molecules as well as **2d**, despite significant contraction in the P-I bond lengths. The only slight difference is a reduced O(1)-P(2) contact observed in one molecule (2.870(3) Å) which results through a minor reduction of the O(1)-C$_{Ar}$C$_P$ and C$_{Ar}$-C$_P$-P(2) angles. This 'pinching' becomes more apparent for [**3e**]I₃ and leads to a significant shortening of the N(2)-P(1) contact (2.845(3) Å *vs*. 2.945(3) Å and 2.933(2) Å for **2e**) as a result of decreased N(2)-C$_{Ar}$-C$_P$ and C$_{Ar}$-C$_P$-P(1) angles. The remaining bond lengths and angles observed in [**3e**]I₃ do not differ from the parent Ar₃PI₂ adduct. The reduced N(2)-P(1) contact suggests that the strength of the N-P-I $3c4e^-$ hypervalent bond increases for the iodophosphonium salt.
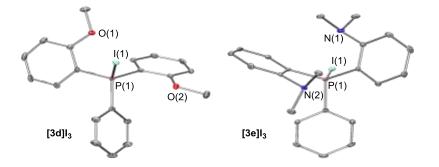

Figure 5: Cationic structures of [**3d**]I₃ and [**3e**]I₃. Drawn with ellipsoids at 30% probability; hydrogen atoms, counterion and solvents of crystallisation omitted for clarity.

In the two structural characterised donor-functionalised iodophosphonium triiodides, the close contacts between the phosphorus-bound iodine and the terminal atom of an I₃⁻ anion lie within the sum of the van der Waals radii (3.96 Å).[30] These covalent interactions results in a weakening

of the P-I bond and lead to increased P-I bond lengths in comparison to the BAr^F salts. [**3d**]I$_3$

adopts a Z-shaped motif structural isomer[55] in which two crystallographically distinct [Ar$_3$PI]$^+$

fragments strongly interact with opposite ends of a single I$_3^-$ anion. The closest contacts between

bridging and interstitial I$_3^-$ anions in [**3d**]I$_3$ are *via* the terminal atoms (4.5359(6) Å and

4.6707(6) Å); this distance is considerably longer than the sum of van der Waals radii and the I-I

contacts observed in the analogous (Ph$_3$PI)I$_3$ polymorph.[54]

Compounds [**3e**]I$_3$ crystallises such that each Ph$_3$PI$^+$ fragment interacts strongly with a single I$_3^-$

anion (3.5802(4) Å). The opposing end of the asymmetric triiodide anion also shows close, likely

dipolar contacts to the NMe$_2$ hydrogens on an adjacent Ph$_3$PI$^+$ fragment (closest contact *ca.*

3.041 Å, within the sum of the C-I van der Waals radii, 3.57 Å) and the aryl protons of an

independent Ph$_3$PI$^+$ fragment (closest contact *ca.* 3.254 Å) but does not appear to interact with

any additional phosphorus-bound iodine atoms or I$_3^-$ anions.

The attempted syntheses of [**3c**]I$_3$ revealed the formation of an unexpectedly downfield ^{31}P NMR

signal which did not correspond to an iodophosphonium salt. Whilst a pure sample of product

could not be isolated, slow diffusion of Et$_2$O into the reaction mixture allowed the isolation of a

few crystals of [**4**]I$_3$ suitable for single crystal diffraction which showed a cyclic phosphonium

salt (Figure 6) in which the NMe$_2$ donor moiety has undergone demethylation to form an amide

species with a formal P-N single bond (1.636(5) Å). This must presumably occur with

concomitant formation of iodomethane in a nitrogen analogue of Michaelis-Arbuzov

chemistry,[58] and implies that the degree of N-P binding on formation of [**3c**] is significantly

increased in comparison to **2c**.

The attempted syntheses of [**3c**]BAr^F gave rise to mixtures with multiple phosphorus containing

species, including a signal assigned to [**4**]BAr^F; this additional complexity is attributed to

subsequent reactions with the MeI formed *in situ* in the presence of the more weakly coordinating anion (See SI for further details).
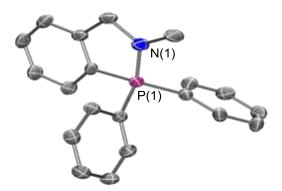

Figure 6: Cationic structure of [**4c**]I$_3$. Drawn with ellipsoids at 50% probability; hydrogen atoms and counterion omitted for clarity.

Computational Investigation

Bonding and Lewis Basicity of Donor-Functionalised Phosphanes

Computational studies were performed to provide further insight into the mechanism by which the apparent donor strength of the phosphanes varies between diiodophosphoranes and iodophosphonium salts. Initial calculations using the LanL2DZ[59,60] effective core potential (ECP) to model the iodine atoms gave poor correlations with observed experimental data, and so the more computationally demanding def2TZVP split valence, triple zeta basis set was employed. This gave reasonable correlation with experimental structural data.

The counter intuitive weakness observed experimentally for the diiodophosphoranes clearly reflects the delicate balance between electronic and steric effects in the adducts. These factors were quantified by examining the energy of the HOMO of the free phosphanes, which in all

cases was found to correspond to an orbital with considerable phosphorus lone pair character and, through buried volume analysis[61-63] (%V_{Bur}) of the optimised Ar_3PI_2 adducts; these can be compared to the I-I bond length as a measure of overall donor strength. Neglecting steric effects, phosphanes with a less negative HOMO energy should, in principle, be stronger donors relative to PPh_3 resulting in an elongation of the I-I distance in the corresponding diiodophosphorane.

	HOMO Energy (eV)	%V_{Bur}	D-P Distance / Å	D-P Bond Index	C_{Ar}-D Distance / Å	C_{Ar}-D Bond Index
1a[c]	-0.26785	23.5	2.852	0.046	1.356	1.049
1b[c]	-0.26476	26.2	2.888	0.063	1.436	1.018
1c[c]	-0.26169	28.8	2.878	0.049	1.453	0.964
1d[c]	-0.26346	25.2	2.857[a]	0.047[a]	1.357[a]	1.046[a]
			2.846[b]	0.043[b]	1.357[b]	1.052[b]
1e[c]	-0.25693	27.3	2.945[a]	0.051[a]	1.430[a]	1.032[a]
			2.890[b]	0.063[b]	1.436[b]	1.019[b]
1g[c]	-0.27296	21.8				
Anisole[c]					1.358	1.065
DMA[c]					1.383	1.077

Table 3: Selected parameters for the computed free phosphanes, showing calculated separations and Mayer Bond indices for Donor-P contacts and the Donor-Arene bonds. [a] For donor involved in D-P-C primary hypervalent bonding motif. [b] For donor involved in D'-P-C secondary hypervalent bonding motif.

The computational studies also confirm that two possible modes exist by which phosphane donor strength is enhanced, namely π-conjugation and direct lone pair donation to phosphorus, and allows clear differences to be established for the oxygen and nitrogen donors. Examination of

the bond indices between the donor atoms and the phosphorus centre, and comparing the occupied molecular orbitals of the free phosphanes provides good evidence for the origin of the different behaviour. Computational structures are referred to with a superscript C to differentiate them from experimental results.

Table 3 shows the clear trend that substitution leads to an increase in both HOMO energy and steric demand of the phosphane as seen in the increase in calculated buried volumes. At the same time, the nitrogen-donors show a greater increase in steric demand than the oxygen donors which may be understood in terms of the coplanarity of the OMe fragments with the arene rings as compared to the twisting out of the the ring plane seen for the nitrogen fragments. Examination of the C_{Ar}-O bond lengths and Mayer bond indices for **1a**[C] (dC$_{Ar}$O 1.356 Å, bond index 1.049) and **1d**[C] (dC$_{Ar}$O 1.357 and 1.357 Å, bond indices 1.046 and 1.052) confirm the presence of π-donation of the oxygen lone pairs into the arene rings (bond indices > 1), albeit with a slight reduction in C_{Ar}-O bond index compared to free anisole (1.065), likely as a result of steric congestion. Nevertheless, the calculated P-O bond indices are low (**1a**[C]: 0.046; **1d**[C]: 0.047 and 0.043) despite the close P-O contacts. In contrast, the orientations of the nitrogen lone pairs in **1b**[C] and **1e**[C] preclude such conjugation and the NMe$_2$ fragments would thus be expected to act as electron withdrawing groups via the σ-bonding network – a significant increase in bond length (**1b**[C]: dC$_{Ar}$N 1.436 Å, bond index 1.018; **1e**[C]: dC$_{Ar}$N 1.430 and 1.436 Å, bond indices 1.032 and 1.019) and decrease in bond indices is observed as compared to free N,N-dimethylaniline (dC$_{Ar}$N 1.383 Å, Bond index 1.077). The nitrogen lone pair of **1b**[C], **1c**[C] and **1e**[C] are all oriented towards the phosphorus centre, as seen in available crystallographic data[64,65] with comparatively short P-N contacts (**1b**[C]: 2.887 Å; **1c**[C]: 2.878 Å; **1e**[C]: 2.945 and 2.890 Å). The energy change of the lone pair must therefore, as previously reported,[8] arise from a small but signifiant degree of N-P

bonding leading to rehybridisation at phosphorus – this is reflected in the calculated N-P bond indices (**1b**[C]: 0.063; **1c**[C]: 0.049; **1e**[C]: 0.051 and 0.063) and in each case, the HOMO-1 is identified as showing P-N σ-bonding character (see SI). Ligand **1c**[C] shows both greater buried volume and a higher energy lone pair than **1b**[C], which may be understood as arising from the transition towards a pseudo-trigonal bipyramidal, five-coordinate geometry; the impact of this rehybridisation may be seen in that the lone pair of **1c**[C] is raised above that of **1d**[C], despite the presence of two strongly conjugated donor moeties in the latter case.

	Bond Lengths / Å				Bond Indices			
	P-I	I-I	D-P	D'-P	P-I	I-I	D-P	D'-P
2a[C]	2.483	3.173	2.858		0.929	0.332	0.037	
2b[C]	2.485	3.150	2.889		0.930	0.350	0.065	
2c[C]	2.491	3.149	2.943		0.925	0.350	0.075	
2d[C]	2.484	3.193	2.876	2.856[a]	0.930	0.314	0.036	0.037[a]
2e[C]	2.467	3.244	2.906	2.971[b]	0.987	0.272	0.061	0.059[b]
2g[C]	2.487	3.138			0.921	0.361		

Table 4: Selected bond lengths and bond indices for the computed diiodophosphoranes, showing calculated separations and Mayer Bond indices for Donor-P contacts and the Donor-arene bonds. [a] Donor involved in D'-P-C secondary hypervalent bonding motif. [b] Donor involved in D'-P-I secondary hypervalent bonding motif.

Geometry optimisation of the diiodophosphoranes confirmed the increase in donor strength of the phosphanes, with increased I-I bond lengths relative to **2g**[C] seen for all cases and shorter P-I contacts for all save **2c**[C], as shown in Table 4. The same trend is seen in the P-I and I-I Mayer bond indices, though here the P-I bond index is nevertheless increased for **2c**[C] relative to **2g**[C], showing that the P-I bond extension arises from steric grounds. Considering first the mono-

substituted phosphorane series, the trends clearly show that despite the increase in lone pair energy indicating an expected donor strength of $\mathbf{1c^C} > \mathbf{1b^C} > \mathbf{1a^C}$, instead $\mathbf{1a^C} > \mathbf{1b^C} \sim \mathbf{1c^C}$ is found by both I-I bond length and bond index comparison (the experimentally observed order is $\mathbf{1a} > \mathbf{1c} > \mathbf{1b}$ by I-I contacts in $\mathbf{2}$). This trend in donor strength instead follows the order dictated by the steric demand of the phosphane as measured by buried volume, with longer P-I and shorter I-I bonds as buried volume increases. Further substitution leads to a proportionately smaller change in buried volume, and so unsurprisingly donor strength is found to increase such that $\mathbf{1d^C} > \mathbf{1a^C}$ and $\mathbf{1e^C} > \mathbf{1b^C}$. Interestingly, despite the increase in donor strength seen in the increase in I-I bond lengths (3.192 Å vs 3.173 Å) and decrease in I-I bond indices (0.314 vs 0.332) for $\mathbf{2d^C}$ relative to $\mathbf{2a^C}$, the P-I bond lengths and bond indices are essentially invariant, confirming that this metric is more sensitive to steric demand than the I-I contact.

On binding of I_2, the computed P-O bond indices decrease for $\mathbf{2a^C}$ and $\mathbf{2d^C}$ relative to the free phosphanes (*e.g.* $\mathbf{2a^C}$: 0.037 *vs* $\mathbf{1a^C}$: 0.046) whilst the C_{Ar}-O bond indices increase, demonstrating that conjugation through the arene rings dominates over direct donation to phosphorus in these systems, whilst an increase in P-N bond index is observed for the mono-substituted nitrogen donor species. This increase is comparatively small for $\mathbf{2b^C}$ ($\mathbf{2b^C}$: 0.065 *vs* $\mathbf{1b^C}$: 0.063), but substantially larger for $\mathbf{2c^C}$ ($\mathbf{2c^C}$: 0.075 *vs* $\mathbf{1c^C}$: 0.049), despite both $\mathbf{2b^C}$ and $\mathbf{2c^C}$ showing a simultaneous increase in P-N bond length (ΔdP-N $\mathbf{2b^C}$: 0.001 Å; $\mathbf{2c^C}$ 0.065 Å). The increase in P-N separation likely arises from the increased steric bulk about phosphorus, but this is concommitant with a change in bond angle towards linearity ($\mathbf{2c^C}$ N-P-C$_{apical}$ angle: 171.4° to 177.1°) which nevertheless improves orbital overlap and thus bonding. For the doubly-substituted donors, the same trends are evident, albeit with a slight decrease observed for the N-P contact in the N-P-I hypervalent interaction of $\mathbf{2e^C}$. Overall, it can therefore be seen that whilst

the internal solvation might be predicted to have a greater influence on donor strength than more remote conjugation, the steric demands imposed by the P-N bonding weaken the effect, with the bonding in $2c^C$ indicating that $1c^C$ is the weakest of the substituted donors despite having the second greatest lone pair energy. $2c^C$ not only shows the smallest increase in I-I separation but also manifests a P-I contact slightly greater in length than that of $2g^C$ ($2c^C$: 2.491 Å *vs* $2g^C$: 2.487 Å).

	Bond Lengths / Å			Bond Indices		
	P-I	D-P	D'-P	P-I	D-P	D'-P
$3a^C$	2.399	2.886		1.036	0.039	
$3b^C$	2.393	2.904		1.047	0.070	
$3c^C$	2.398	2.949		1.044	0.088	
$3d^C$	2.403	2.886	2.859[a]	1.029	0.038	0.040[a]
$3e^C$	2.410	2.915	2.858[b]	1.056	0.064	0.083[b]
$3g^C$	2.392			1.040		

Table 5: Selected bond lengths and bond indices for the computed iodophosphonium cations, showing calculated separations and Mayer Bond indices for Donor-P contacts and the Donor-Arene bonds. [a] Donor involved in D'-P-C secondary hypervalent bonding motif. [b] Donor involved in D'-P-I secondary hypervalent bonding motif.

The optimised iodophosphonium series, shown in Table 5, however, tells a very different story in that all of the substituted cations exhibit longer P-I bonds than $3g^C$ (although nevertheless still all shorter than the P-I contacts seen in the diiodophosphoranes), implying weaker donor strength and the reverse of the trend seen for the diiodophosphoranes. Interestingly, whilst the steric demands clearly dominate in this situation, the efficiency of direct P-N donation at enhancing

donor strength can clearly be seen in that the P-I contact of $3c^C$ is essentially identical to that of $3a^C$, despite the enormous increase in steric bulk between $1c^C$ and $1a^C$. Furthermore, the nitrogen donor systems $3b^C$, $3c^C$ and $3e^C$ show P-I bond indices greater than that for $3g^C$, whilst the oxygen donor systems $3a^C$ and $3d^C$ show reduced P-I bond indices. This is mirrored in the bond indices for C_{ortho}-O, P-O and P-N contacts. The P-O bond indices for $3a^C$ (0.039) and $3d^C$ (0.038 and 0.040) do show an increase relative to the diiodophosphoranes, but do not rise to the levels seen in the free phosphanes, and there is also a significant increase in C_{ortho}-O bond index ($3a^C$: 1.084; $3d^C$: 1.079 and 1.081) commensurate with a greater degree of charge transfer to phosphorus through the arene ring. The P-N bonds indices for $3b^C$, $3c^C$ and $3e^C$, ($3b^C$: 0.070; $3c^C$: 0.088; $3e^C$: 0.064 and 0.083) on the other hand, are increased relative to the diiodophosphoranes, with the greatest increase seen for $3c^C$ despite a slight associated increase in bond length (ΔdP-N $3c^C$ 0.005 Å). Unfortunately, since complete crystallographic data could not be obtained for either I_3^- or BAr^F salts, it is not possible to directly and generally compare computational and experimental results, though the invariance of the P-I bond length observed for [3]BAr^F suggests that packing effects, not computationally modelled, may be significant.

The computational results give good correlation with experimental data and allow the relative donor strength of the donor substituted phosphanes to be explained in terms of electronic and steric effects. However, the apparent dramatically weak Lewis basicity observed experimentally in $2b$, which could not be fully predicted computationally, suggests that there is an additional factor to consider. The crystal packing of the Ar_3PI_2 adducts will also influence the observed donor strength since favourable supramolecular interactions will alter the conformation and orientation of the aryl rings which in turn affects the magnitude of the P-I and I-I bond lengths.[25] Out of the six crystallographically characterised diiodophosphoranes, $2b$ is the only

diiodophosphorane in which the back-to-back sextuple phenyl embrace is observed. This conformation is commonly adopted for Ph$_3$P containing species[66] and contains six attractive edge-to-face (EF) interactions between aryl groups and contributes to a significant attraction between molecules. Given that this intermolecular embrace is only seen for **2b**, and since crystal packing has not been considered computationally, it is plausible that this is responsible for the long P-I and short I-I bond lengths observed experimentally for this adduct.

Conclusions

Analysis of the reported diiodophosphoranes, supplemented by computational studies, shows that the phosphorus centres of these nitrogen-donor substituted phosphanes are themselves internally solvated and may act simultaneously as Lewis acid and Lewis base. In contrast, no significant internal solvation is observed for the oxygen-donor substituted phosphanes, with their increased donor ability arising from localisation of oxygen lone pairs onto phosphorus *via* an aromatic system. Comparison of the I$_2$ adduct structures reveals a counter intuitively weak Lewis basicity for **1c**, indicated by a decrease in the I-I bond length when compared to the unsubstituted PPh$_3$ donor, shown to derive from a delicate balance between steric and electronic effects within the adducts. Synthesis of the corresponding iodophosphonium salts, in tandem with further computational studies, reveals that the impact of the steric bulk on donor strength is more significant for the cationic species but also that in these species internal solvation is more efficient at increasing donor strength than through-ring conjugation. These observations imply that this internal solvation may be general to soft Lewis acid adducts of these donor-functionalised phosphanes, with implications for their utility in stabilising main group cations – the assumption that more donor substituents leads to better cation stabilisation may not hold. Finally, the marked difference in behaviour between neutral adduct and cation clearly indicates

35

that, when comparing the donor strength of ligands, a single probe Lewis acid is insufficient to understand the overall trends in ligand behaviour.

Supporting Information

Complete multinuclear NMR data, selected computational results and Cartesian coordinates of all optimised diiodphosphoranes, iodophosphoniums and free phosphanes are available in the supporting information. This material is available free of charge via the Internet at http://pubs.acs.org. The crystallographic data have been submitted to the Cambridge Crystallographic Database (Deposit numbers: 1530537, 1530536, 1530540, 1530541, 1530539, 1530538, 1530491, 1530492, 1530493, 1530490, 1530495, 1530498, 1530496, 1530497).

Corresponding Author

School of Physical Sciences, University of Kent, Ingram Building, Canterbury, Kent, CT2 7NH, UK. E-mail: e.r.clark@kent.ac.uk

Author Contributions

The manuscript was written through contributions of both authors. Both authors have given approval to the final version of the manuscript.

Abbreviations:

BAr^F - tetrakis[3,5-bis(trifluoromethyl)phenyl]borate

CT - charge transfer

DCM - dichloromethane

ECP - effective core potential

Et$_2$O - diethyl ether

EtOH – ethanol

GUI - graphical user interface

HOMO - highest occupied molecular orbital

MeOH – methanol

NBO - natural bond orbital

NMR - nuclear magnetic resonance

PCM - polarisable continuum model

THF - tetrahydrofuran

References

[1] Farrell. J. M, Hatnean. J. A, Stephan. D. W. Activation of Hydrogen and Hydrogenation Catalysis by a Borenium Cation. *J. Am. Chem. Soc.* **2012**, *134* (38), 15728-15731.

[2] Clark. E. R, Ingleson. M. J. [(acridine)BCl$_2$]$^+$: A Borenium Cation That Is a Strong Boron- and Carbon-Based Lewis Acid. *Organometallics.* **2013**, *32* (22), 6712-6717.

[3] Eisenberger. P, Bestvater. B. P, Keske. E. C, Crudden. C. M. Hydrogenations at Room Temperature and Atmospheric Pressure with Mesoionic Carbene-Stabilized Borenium Catalysts. *Angew. Chemie Int. Ed.* **2015**, *54* (8), 2467-2471.

[4] Vom Stein. T, Peréz, Dobrovestsky. R, Winkelhaus. D, Caputo. C. B, Stephan. D. W. Electrophilic Fluorophosphonium Cations in Frustrated Lewis Pair Hydrogen Activation and Catalytic Hydrogenation of Olefins. *Angew. Chemie Int. Ed.* **2015**, *54* (35), 10178-10182.

[5] Ugarte. R. A, Devarajan. D, Mushinski. R. M, Hudnall. T. W. Antimony(V) cations for the selective catalytic transformation of aldehydes into symmetric ethers, α,β-unsaturated aldehydes, and 1,3,5-trioxanes. *Dalton Trans.* **2016**, *45*, 11150-11161.

[6] Hirai. M, Cho. J, Gabbaï. F. P. Promoting the Hydrosilylation of Benzaldehyde by Using a Dicationic Antimony-Based Lewis Acid: Evidence for the Double Electrophilic Activation of the Carbonyl Substrate. *Chem. Eur. J.* **2016**, *22* (19), 6537-6541.

[7] Talavera. G, Peña. J, Alcarazo. M. Dihalo(imidazolium)sulfuranes: A Versatile Platform for the Synthesis of New Electrophilic Group-Transfer Reagents. *J. Am. Chem. Soc.* **2015**, *137* (27), 8704-8707.

[8] Clark. E. R, Borys. A.M, Pearce. K. Donor-substituted phosphanes – surprisingly weak Lewis donors for phosphenium cation stabilisation. *Dalton Trans.* **2016**, *45*, 16125-16129.

[9] See for instance a) Ananthnag. G. S, Edukondalu. N, Mague. J. T, Balakrishna. M. S. Copper and palladium complexes of 2-(diphenylphosphino)-N,N-dimethylbenzylamine and its selenide derivative. *Polyhedron,* **2013**, *62*, 203-207 ; b) Shirakawa. E, Yamamoto. Y, Nakao. Y, Oda. S, Tsuchimoto. T, Hiyama. T. Nickel-Catalyzed Tandem Carbostannylation of Alkynes and 1,2-Dienes with Alkynylstannanes. *Angew. Chem. Int. Ed.* **2004**, *43*, 3448 –3451.

[10] C. Chuit, R. J. P. Corriu, P. Monforte, C. Reyé, J. Declercq and A. Dubourg. The structures of tris (8-dimethylamino-1-naphthy1) phosphane and tris [Z-(dimethylaminomethyl) phenylphosphane: The crystallographic detection of sevenfold coordinated phosphorus. *Angew. Chemie,* **1993**, *105*, 1529-1531.

[11] Weller. F, Nuszhar. D, Dehncke. K, Gingl. F, Strahle. J. On the Reactions of Phosphaneiminato Complexes of Niobium, Molybdenum, and Tungsten with Sodium Fluoride. The Crystal Structures of $[PPh_3NH_2]Cl$ and PPh_3F_2. *Z. Anorg. Allg. Chem.* **1991**, *602*, 7-16.

[12] Godfrey. S. M, McAuliffe. C. A, Pritchard. R. G, Sheffield. J. M, Thompson. G. M. Structure of R_3PCl_2 compounds in the solid state and in solution: dependency of structure on R. Crystal-structures of trigonal bipyramidal $(C_6F_5)_3PCl_2$, $Ph_2(C_6F_5)PCl_2$ and of ionic $Pr^n_3PCl_2$. *J. Chem. Soc., Dalton Trans.* **1997**, 4823-4828.

[13] Godfrey. S. M, McAuliffe. C. A, Sheffield. J. M. Structural dependence of the reagent Ph_3PCl_2 on the nature of the solvent, both in the solid state and in solution; X-ray crystal structure of trigonal bipyramidal Ph_3PCl_2, the first structurally characterised five-coordinate R_3PCl_2 compound. *J. Chem. Soc., Dalton Trans.* **1998**, 921-922.

[14] Al-Juboori. M. A. H. A, Gates. P. N, Muir. A. S. Ionic–molecular isomerism in chlorophenylphosphoranes Ph_nPCl_{5-n} ($1 \leq n \leq 3$). *J. Chem. Soc., Chem. Commun.* **1991**, 1270-1271.

[15] Bricklebank. N, Godfrey. S. M, Mackie. A. G, McAuliffe. C. A, Pritchard. R. G, Watson. J. M. The structure of triphenylphosphorus–dibromine, the first crystallographically characterised bromophosphorane, a compound which has the novel four-coordinate molecular Ph_3P–Br–Br geometry. *J. Chem. Soc., Chem. Commun.* **1992**, 355-356.

[16] Ruthe. F, du Mont. W-W, Jones. P. G. 'Soft–soft' halogen–halogen interactions in solid ion pairs of solvent-free $Pr^i_3PCl_2$ and CH_2Cl_2-solvated $Pr^i_3PBr_2$: structural features of chloro- and bromo-triisopropylphosphonium salts. *Chem. Commun.* **1997**, 1947-1948.

[17] Godfrey. S. M, McAuliffe. C. A, Mushtaq. I, Pritchard. R. G, Sheffield. J. M. The structure of R_3PBr_2 compounds in the solid state and in solution; geometrical dependence on R, the crystal structures of tetrahedral ionic Et_3PBr_2 and molecular trigonal bipyramidal $(C_6F_5)_3PBr_2$. *J. Chem. Soc., Dalton Trans.* **1998**, 3815-3818.

[18] Hrib. C. G, Ruthe. F, Seppälä. E, Bätcher. M, Druckenbrodt. C, Wismach. C, Jones. P. G. du Mont. W-W. Lippolis. V, Devillanova. F. A, Bühl. M. The Bromination of Bulky Trialkylphosphane Selenides $R_2R'PSe$ (R, R′ = *i*Pr or *t*Bu) Studied by Physical and Computational Methods. *Eur. J. Inorg. Chem.* **2006**, 88-100

[19] Du Mont. W-W, Bätcher. M, Pohl. S, Saak. W. Iodophosphonium Salts with Unusual Properties and a Structural Alternative for Halophosphoranes. *Angew. Chem. Int. Ed. Engl.* **1987**, *26*, 912-913.

[20] Godfrey. S. M, Kelly. D. G, Mackie. A. G, McAuliffe. C. A, Pritchard. R. G, Watson. S. M. The Structure of Triphenylphosphorus Diiodine, Ph_3I_2, the 1st Crystallographically Characterized Dihalogen Derivative of a Tertiary Phosphine. *J. Chem. Soc., Chem. Commun.* **1991**, *17*, 1163-1164.

[21] Bricklebank. N, Godfrey. S. M, Lane. H. P, McAuliffe. C. A, Robin G. Pritchard and Moreno. J. M. The Isolation from Diethyl Ether of Ionic [(Me,N),PI]I and [(CH_2=CHCH_2)_2PhPI]I, and the Crystallographically Characterised Molecular 'Spoke' Structure PhMe,PI. *J. Chem. Soc., Dalton Trans.* **1995**, 2421-2424.

[22] Ruthe. F, Jones. P. G, Du Mont. W-W, Deplano. P, Mercuri. M. L. Oxidation of Triisopropylphosphane with Iodine: The Role of Dry or Moist Solvent. *Z. Anorg. Allg. Chem.* **2000**, *626*, 1105-1111.

[23] Godfrey. S. M, McAuliffe. C. A, Pritchard. R. G, Sheffield. J. M. An X-ray crystallorgraphic study of the reagent Ph_3PCl_2; not charge-transfer, $R_3P–Cl–Cl$, trigonal bipyramidal or $[R_3PCl]Cl$ but an unusual dinuclear ionic species, $[Ph_3PCl^+···Cl^-···^+ClPPH_3]Cl$ containing long Cl–Cl contacts. *Chem. Commun.* **1996**, 2521-2522.

[24] Nikitin. K, Müller-Bunz. H, Gilheany. D. Direct evidence of a multicentre halogen bond: unexpected contraction of the P–XXX–P fragment in triphenylphosphine dihalides. *Chem. Commun.* **2013**, *49*, 1434-1436.

[25] Barnes. N. A, Godfrey. S. M, Khan. R. Z, Pierce. A, Pritchard. R. G. A structural and spectroscopic study of *tris*-aryl substituted R_3PI_2 adducts. *Polyhedron*. **2012**, *35*, 31-46.

[26] Teixidor. F, Núñez. R, Viñas. C, Sillanpää. R, Kivekäs. R. The Distinct Effect of the o-Carboranyl Fragment: Its Influence on the I−I Distance in R_3PI_2 Complexes. *Angew. Chem. Int. Ed.* **2000**, *39*, 4290-4292.

[27] Barnes. N. A, Godfrey. S. M, Halton. R. T. A, Mushtaq. I, Pritchard. R. G. The reactions of alkylamino substituted phosphines with I_2 and $(Ph_2Se_2I_2)_2$: structural features of alkylamino phosphonium cations. *Dalton Trans.* **2008**, 1346-1354.

[28] McAuliffe. C. A, Beagley. B, Gott. G. A, Mackie. A. G, MacRory. P. P, Pritchard. R. G. Structure of Triphenylarsane Diiodide, $[Ph_3AsI_2]$, a Compound Formed in the Thermal Decomposition of $[Mn(OAsPh_3)_3I_2(SO_2)_2]$. *Angew. Chem. Int. Ed. Engl.* **1987**, *26*, 264-265.

[29] Wells. A. F. *Structural Inorganic Chemistry*, 5th Ed., Clarendon Press, Oxford, **1984**, pp. 851.

[30] Bondi. A. Van der Waals Volumes and Radii. *J. Phys. Chem.* **1964**, *68* (3), 441-451.

[31] Barnes. N. A, Flower, K. R, Godfrey. S. M, Hurst. P. A, Khan. R. Z, Pritchard. R. G. Structural relationships between *o*-, *m*- and *p*-tolyl substituted R_3EI_2 (E = As, P) and $[(R_3E)AuX]$ (E = As, P; X = Cl, Br, I). *Cryst. Eng. Comm.* **2010**, *12*, 4240-4251.

[32] High precision data collected in this work at 100K. Original P-I and I-I bond metrics[17] at 293K: 2.480(4) Å and 3.161(2) Å respectively.

[33] Barnes. N. A, Godfrey. S. M, Halton. R. T. A, Mushtaq. I., Pritchard. R. G. The reaction of tertiary phosphines with $(Ph_2Se_2I_2)_2$ - the influence of steric and electronic effects. *Dalton Trans.* **2006**, 4795-4804.

[34] McEwen. W. E, Shiau. W-I, Yeh. Y-I, Schulz. D. N, Pahilagn. R. U, Levy. J. B, Symmes. C, Nelson. G. O, Granoth. I. Chemical and physical consequences of 2p-3d overlap in *o*-anisylphosphines and *o*-anisylphosphonium salts. *J. Am. Chem. Soc.* **1975**, *97* (7), 1787-1794.

[35] Cairns. S. M, McEwen. W. E. Contrasting chemical and physical properties of [*o*- and [*p*-(N,N-dimethylamino) phenyl]phosphines and phosphonium salts. *Heteroat. Chem.* **1990**, *1* (1), 9-19.

[36] Keldsen. G. L, McEwen. W. E. Chemical consequences of through space 2p-3d overlap in the alkaline cleavage of benzyltriarylphosphonium chlorides. *J. Am. Chem. Soc.* **1978**, *100* (23), 7312-7317.

[37] Dolomanov. O. V, Bourhis. L. J, Gildea. R. J, Howard. J. A. K, Puschmann. H. OLEX2: a complete structure solution, refinement and analysis program. *J. Appl. Cryst.* 2000, *42*, 339-34.1

[38] Sheldrick. G. M. SHELXT – Integrated space-group and crystal structure determination. *Acta. Cryst.* **2015**, *A71*, 3-8.

[39] Sheldrick. G. M. Crystal structure refinement with SHELXL. *Acta. Cryst.* **2015**, *C71*, 3-8.

[40] Farrugia. L. J. *ORTEP*-3 for Windows – a version of *ORTEP*-III with a Graphical User Interface (GUI). *J. Appl. Crystallogr.* **1997**, *37*, 565.

[41] Gaussian 09, Revision D.01, M. J. Frisch, G. W. Trucks, H. B. Schlegel, G. E. Scuseria, M. A. Robb, J. R. Cheeseman, G. Scalmani, V. Barone, B. Mennucci, G. A. Petersson, H. Nakatsuji,

M. Caricato, X. Li, H. P. Hratchian, A. F. Izmaylov, J. Bloino, G. Zheng, J. L. Sonnenberg, M. Hada, M. Ehara, K. Toyota, R. Fukuda, J. Hasegawa, M. Ishida, T. Nakajima, Y. Honda, O. Kitao, H. Nakai, T. Vreven, J. A. Montgomery, Jr., J. E. Peralta, F. Ogliaro, M. Bearpark, J. J. Heyd, E. Brothers, K. N. Kudin, V. N. Staroverov, R. Kobayashi, J. Normand, K. Raghavachari, A. Rendell, J. C. Burant, S. S. Iyengar, J. Tomasi, M. Cossi, N. Rega, J. M. Millam, M. Klene, J. E. Knox, J. B. Cross, V. Bakken, C. Adamo, J. Jaramillo, R. Gomperts, R. E. Stratmann, O. Yazyev, A. J. Austin, R. Cammi, C. Pomelli, J. W. Ochterski, R. L. Martin, K. Morokuma, V. G. Zakrzewski, G. A. Voth, P. Salvador, J. J. Dannenberg, S. Dapprich, A. D. Daniels, Ö. Farkas, J. B. Foresman, J. V. Ortiz, J. Cioslowski, D. J. Fox, Gaussian, Inc., Wallingford CT, 2009.

[42] Zhao. Y, Truhlar, D. G. The M06 suite of density functionals for main group thermochemistry, thermochemical kinetics, noncovalent interactions, excited states, and transition elements: two new functionals and systematic testing of four M06-class functionals and 12 other functionals. *Theor. Chem. Account.* **2008**, *120*, 215-241.

[43] Weigend. F, Ahlrichs. R. Balanced basis sets of split valence, triple zeta valence and quadruple zeta valence quality for H to Rn: Design and assessment of accuracy. *Phys. Chem. Chem. Phys*. **2005**, *7*, 3297-305.

[44] McLean. A. D, Chandler. G. S. Contracted Gaussian-basis sets for molecular calculations. 1. 2nd row atoms, Z=11-18. *J. Chem. Phys.* **1980**, *72*, 5639-48.

[45] http://comp.chem.umn.edu/info/DFT.htm

[46] NBO Version 3.1, E. D. Glendening, A. E. Reed, J. E. Carpenter, and F. Weinhold.

[47] Bridgeman. A. J, Cavigliasso. G, Ireland. L. R, Rothery. J. The Mayer bond order as a tool in inorganic chemistry. *J. Chem. Soc., Dalton Trans.* **2001**, 2095-2108.

[48] Sizova. O. V, Skripnikov. L. V, Sokolov. A. Y. Symmetry decomposition of quantum chemical bond orders. *J. Mol. Struct*. **2008**, *870*, 1-9.

[49] Lu. T, Chen. F. Multiwfn: A Multifunctional Wavefunction Analyzer. *J. Comp. Chem.* **2012**, *33*, 580.

[50] Seidel. R. W, Goddard. R. Anisole at 100 K: the first crystal structure determination. *Acta Cryst.* **2015**, *C71*, 664-666.

[51] Allen. F. H, Kennard. O, Watson. D. G, Brammer. L, Orpen. A. G, Taylor. R. Tables of bond lengths determined by *X*-ray and neutron diffraction. Part 1. Bond lengths in organic compounds. *J. Chem. Soc., Perkin Trans. 2*, **1987**, S1-S19.

[52] Godfrey. S. M, McAuliffe. C. A, Pritchard. R. G, Sheffield. M. The synthesis and characterisation of R_3PXCN [R = 2,4,6-$(CH_3O)_3$-C_6H_2, 2,6-$(CH_3O)_2C_6H_3$, $NCCH_2CH_2$, C_6H_{11} or $PhCH_2$; X = Br or I] in the solid state and in solution. *Dalton Trans.* **1998**, 1919-192

[53] Deplano. P, Godfrey. S. M, Isaia. F, McAuliffe. A. C, Mercuri. M. L, Trogu. E. F. Tertiary Phosphane-Diiodine Compounds: Are They Molecular Adducts or Iodophosphonium Iodides?

Chem. Ber. **1997**, *130*, 299-305.

[54] Cotton. F. A, Kibala. A. P. Reactions of Iodine with Triphenylphosphine and Triphenylarsine. *J. Am. Chem. Soc.* **1987**, *109* (11), 3308-3312.

[55] Alhanash. F. B, Barnes. N. A, Godfrey. S. M, Hurst. P. A, Hutchinson. A, Khan. R. Z, Pritchard. R. G. Structural isomerism in tris-tolyl halo-phosphonium and halo-arsonium tri-halides, [(CH$_3$C$_6$H$_4$)$_3$EX][X$_3$], (E = P, As; X = Br, I). *Dalton Trans.* **2012**, *41*, 7708-7728.

[56] Trotter. J. A three-dimensional analysis of the crystal structure of p-benzoquinone. *Acta Cryst.* **1960**, *13*, 86-95.

[57] Wilson. C. C, Shankland. N, Florence. A. J. A single-crystal neutron diffraction study of the temperature dependence of hydrogen-atom disorder in benzoic acid dimers. *J. Chem. Soc.* **1996**, *92*, 5051-5057.

[58] Bhattacharya. A. K, Thyagarajan. G. The Michaelis-Arbuzov rearrangement. *Chem. Rev.* **1981**, *81* (4), pp 415–430,

[59] Wadt. W. R, Hay. P. J. Ab initio effective core potentials for molecular calculations - potentials for main group elements Na to Bi. *J. Chem. Phys.* **1985**, *82*, 284-98.

[60] Hay. P. J, Wadt. W. R. Ab initio effective core potentials for molecular calculations - potentials for K to Au including the outermost core orbitals. *J. Chem. Phys.* **1985**, *82*, 299-310.

[61] Poater. A, Ragone. F, Giudice. S, Costabile. C, Dorta. R, Nolan. S. P, Cavallo. L. Thermodynamics of N-heterocyclic carbene dimerization: The balance of sterics and electronics. *Organometallics*. **2008**, *27*, 2679-2681.

[62] Poater. A, Cosenza. B, Correa. A, Giudice. S, Ragone. F, Scarano. V, Cavallo. L. SambVca: A Web Application for the Calculation of the Buried Volume of N-Heterocyclic Carbene Ligands. *Eur. J. Inor. Chem.* **2009**, 1759-1766.

[63] Although typically used for N-heterocyclic carbene ligands, buried volume analysis allows the relative sterics within the six diiodophosphoranes and corresponding iodophoshoniums to be compared internally. Parameters applied for SambVca calculations: 3.50Å was selected as the value for the sphere radius, Bondi radii were unscaled and hydrogen atoms were included.

[64] Suomalainen. P, Jääskeläinen. S, Haukka. M, Laitinen. R. H, Pursiainen. J, Pakkanen. T. A. Structural and Theoretical Studies of ortho-Substituted Triphenylphosphane Ligands and Their Rhodium(I) Complexes. *Eur. J. Inorg. Chem.* **2000**, 2607-2613.

[65] Mudalige. D. C, Ma. E. F. F, Rettig. S. J, Patrick. B. O, James. B. R. Ruthenium(III) complexes containing bi- and tridentate phosphorus−nitrogen ligands. *Can. J. Chem.* **2014**, *92* (8), 716-723.

[66] Dance. I, Scudder. M. The Sextuple Phenyl Embrace, a Ubiquitous Concerted Supramolecular Motif. *J. Chem. Soc., Chem. Commun.* **1995**, 1039-1040.

Table of Contents Synopsis: *ortho*-Donor substituted triarylphosphanes are chelating ligands when bound to transition metals, but monodenate donors when binding the soft Lewis acid I_2 to give charge-transfer complexes. The donor substituents nevertheless increase the donor strength of the phosphane, but by two distinct mechanisms. Oxygen donors enhance donor strength by π-conjugation of lone pairs via the arene, whilst nitrogen donors internally solvate the phosphorus donor, leading to simultaneous Lewis acidity and basicity at phosphorus.

For Table of Contents Only: